Università degli Studi di Ferrara

DOTTORATO DI RICERCA IN FISICA

CICLO XXVIII

Advanced modeling for studying antineutrinos and gamma rays coming from the Earth

Graduate Student

Virginia Strati

Tutors

Prof. Giovanni Fiorentini

Prof. Fabio Mantovani

PhD Dissertation - Ferrara, 18 March 2016

Summary of my research experience

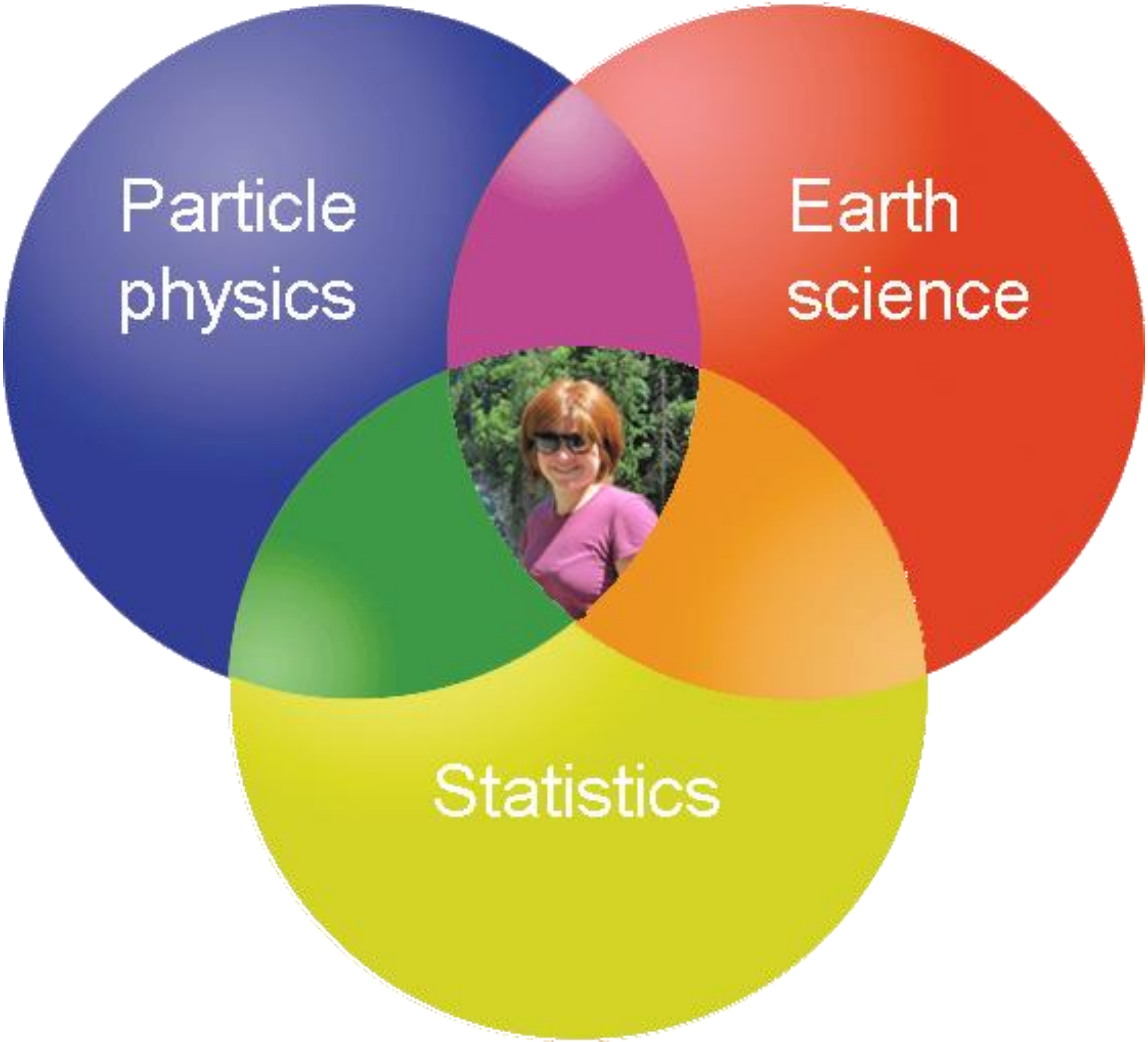

How much uranium is in the Earth?

The answer provides clues to solve other fundamental questions:

• **What is the radiogenic contribution to the heat flow?**

COSMOCHEMICAL MODEL

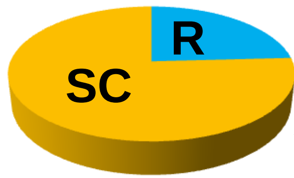

M_U = 5 x10^{16} kg
Radiogenic = **11 TW**
Secular **C**ooling ~ 36 W

GEOCHEMICAL MODEL

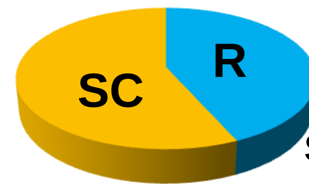

M_U = 8 x10^{16} kg
Radiogenic = **20 TW**
Secular **C**ooling ~ 27 W

• **Which are the building blocks (chondritic meteorites) used to make the planet?**

Enstatites Chondrites

A_U = 12 ppb
Th/U = 3.6

Carbonaceous Chondrites

A_U = 20 ppb
Th/U = 4

• **What kind of mechanical and thermal processes affected the early stages of the Earth formation?**

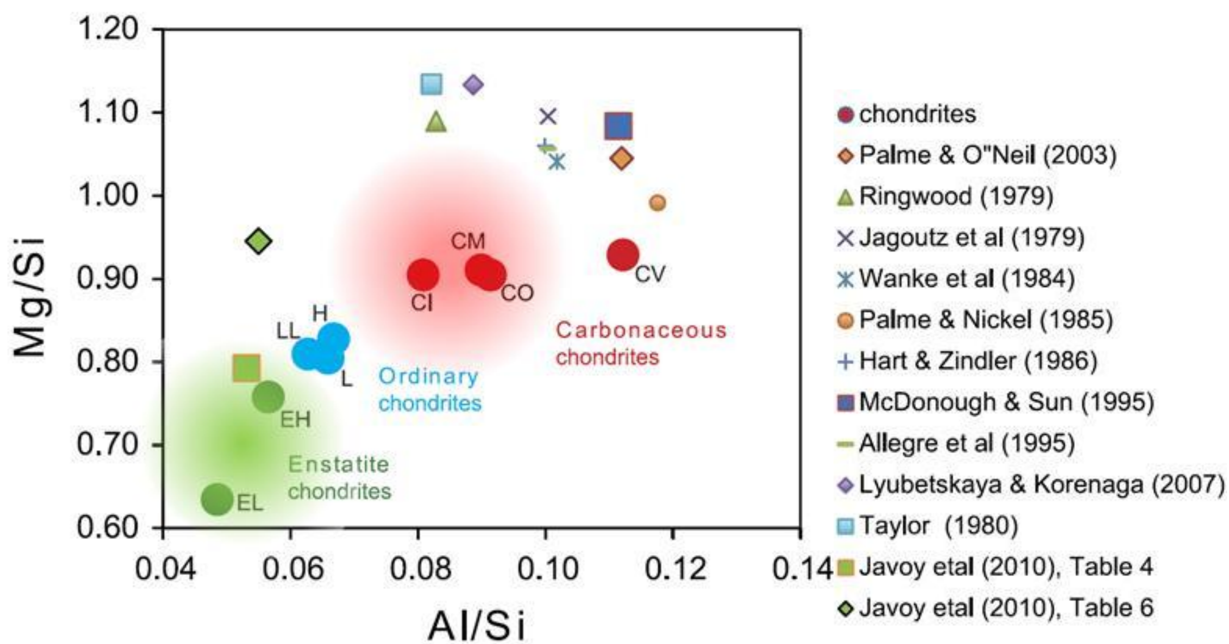

How to measure uranium?


The **terrestrial radioactivity,** due mainly to the presence of ^{238}U, ^{232}Th and ^{40}K, can be considered a probe to study the Earth.

	Type of decays	$T_{1/2}$ [Gyr]	ε_ν [$kg^{-1}s^{-1}$]	Q [MeV]	ε_H [μW/kg]
^{238}U	**α, β, βγ**	**4.5**	**7.46 x 10^7**	**51.7**	**95**
^{232}Th	α, β, βγ	14.0	1.62 x 10^7	42.7	27
^{40}K	βγ (89%)	1.3	2.32 x 10^8	1.3	22

• A fraction of electron antineutrinos produced in β decays along the ^{238}U and ^{232}Th decay chains, i.e. **geoneutrinos**, can be revealed.

• ^{40}K and some daughter nuclides of ^{238}U and ^{232}Th emit **γ- rays** having energy ~ MeV which can be easily detected.

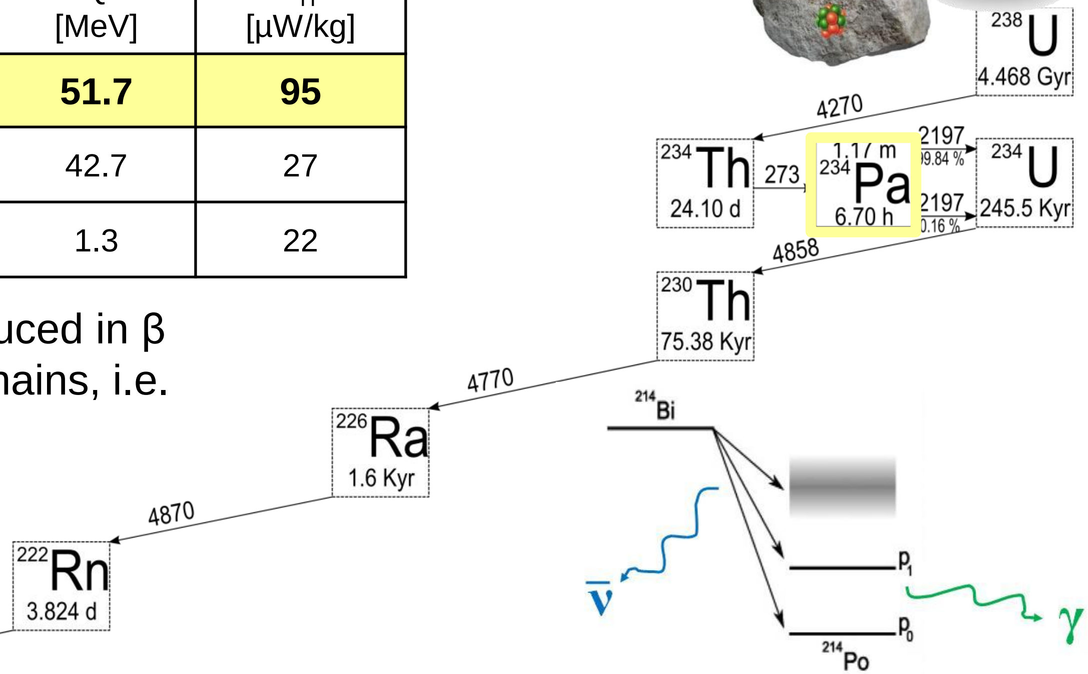

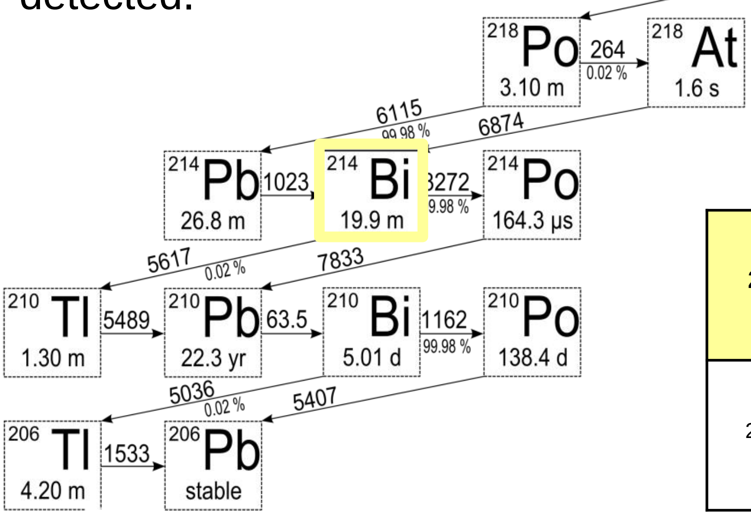

		Effective $\bar{\nu}$		Effective γ	
		E_{max} (MeV)	Signal	E(MeV)	Relative Intensity
^{238}U	**^{234m}Pa**	**2.27**	**31 %**	**1.00**	**0.8 %**
	^{214}Bi	**3.27**	**48 %**	**0.61**	**45.5 %**
^{232}Th	^{212}Bi	2.25	20 %	0.73	6.6 %
	^{228}Ac	2.07	1 %	0.91	26.2 %

^{214}Bi decay detected with gamma and antineutrinos

Antineutrino spectra from the highest βγ decays

The antineutrino spectrum originated by ^{214}Bi is continue and the end point is given by:

$$E_{\bar{\nu}} = Q - T_e - E_\gamma$$

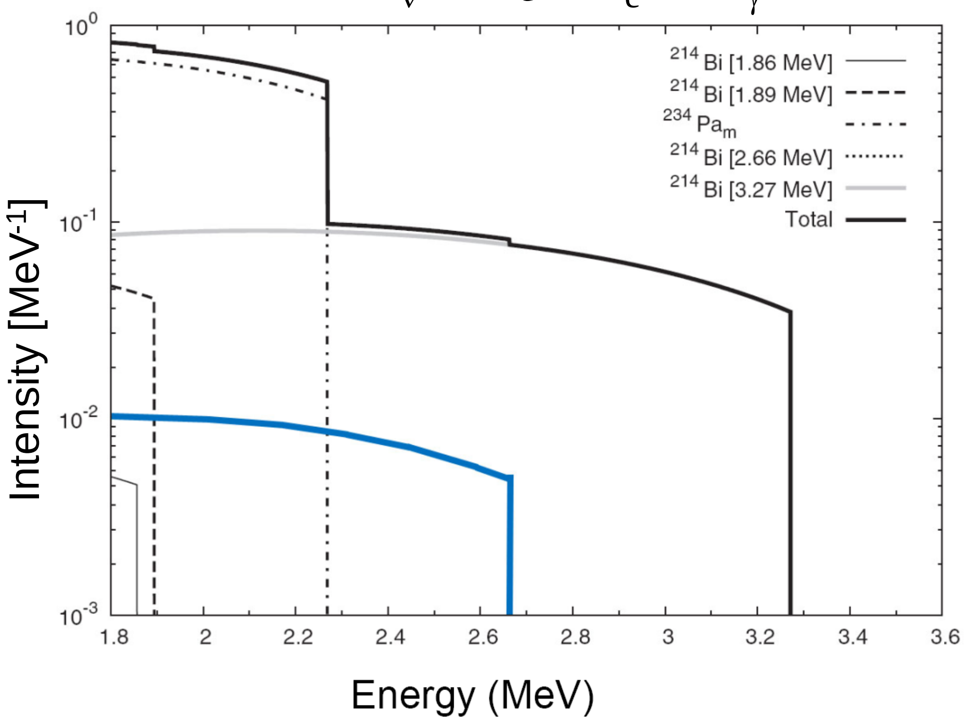

Highest γ-ray emission line spectra

The energy of gamma lines is monochromatic and depends on nuclear transition:

$$E_\gamma = Q - \left(E_{\bar{\nu}} + T_e\right)$$

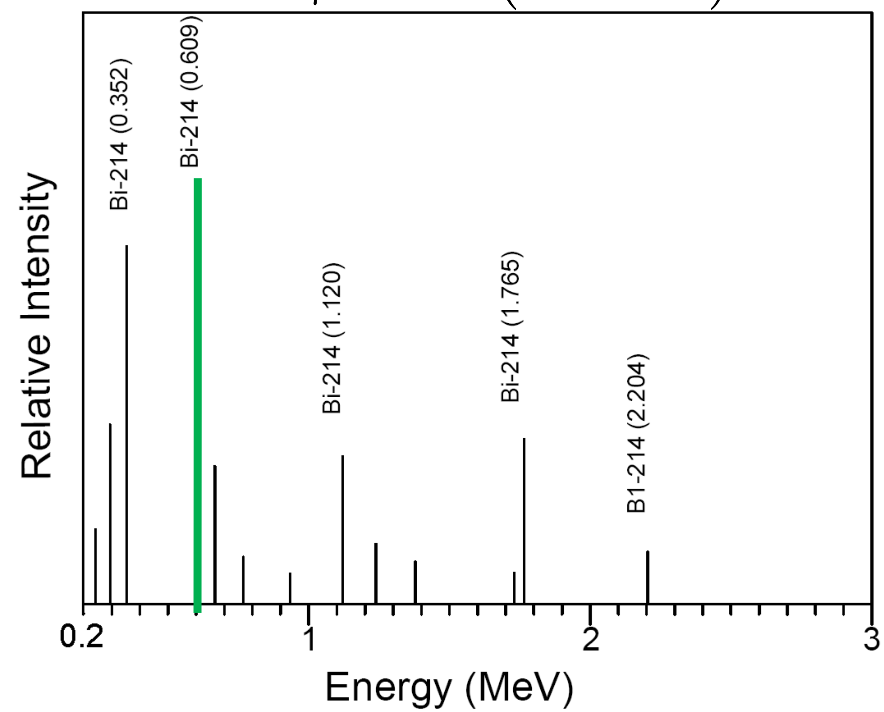

- **Q = 3.27 MeV**
- **82 excited ^{214}Po states**

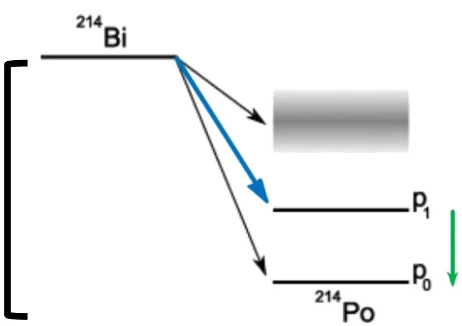

$$^{214}Bi \rightarrow {}^{214}Po^* + e + \bar{\nu}_e$$

2.66 MeV

$$^{214}Po^* \rightarrow {}^{214}Po + \gamma$$

609 KeV

This βγ transition produces detectable geoneutrinos and gamma ray

Different ways of detection

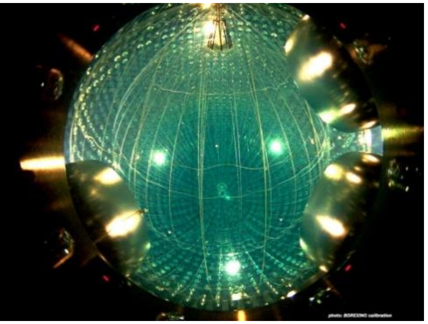


$\bar{\nu}$

- Liquid Scintillator (LS) detector (~ kton)

INVERSE BETA REACTION

$$\bar{\nu} + p \rightarrow e^{+} + n - 1.8\ \text{MeV}$$

- Delayed coincidence of two flashes of light identifies an antineutrino event.





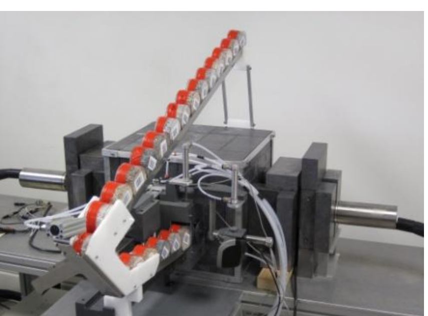
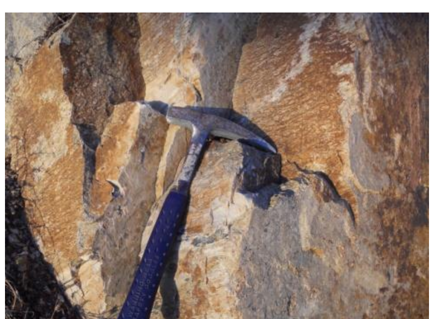

γ

GAMMA RAYS SPECTROSCOPY

Identification and quantification of radionuclides.

Sodium iodide (NaI) detectors

- Scintillation detectors
- High efficiency and good spectral resolution
- Ground and airborne surveys

Hyper Pure Germanium (HPGe) detectors

- Semiconductors detectors
- High energetic resolution
- Rock and soils samples

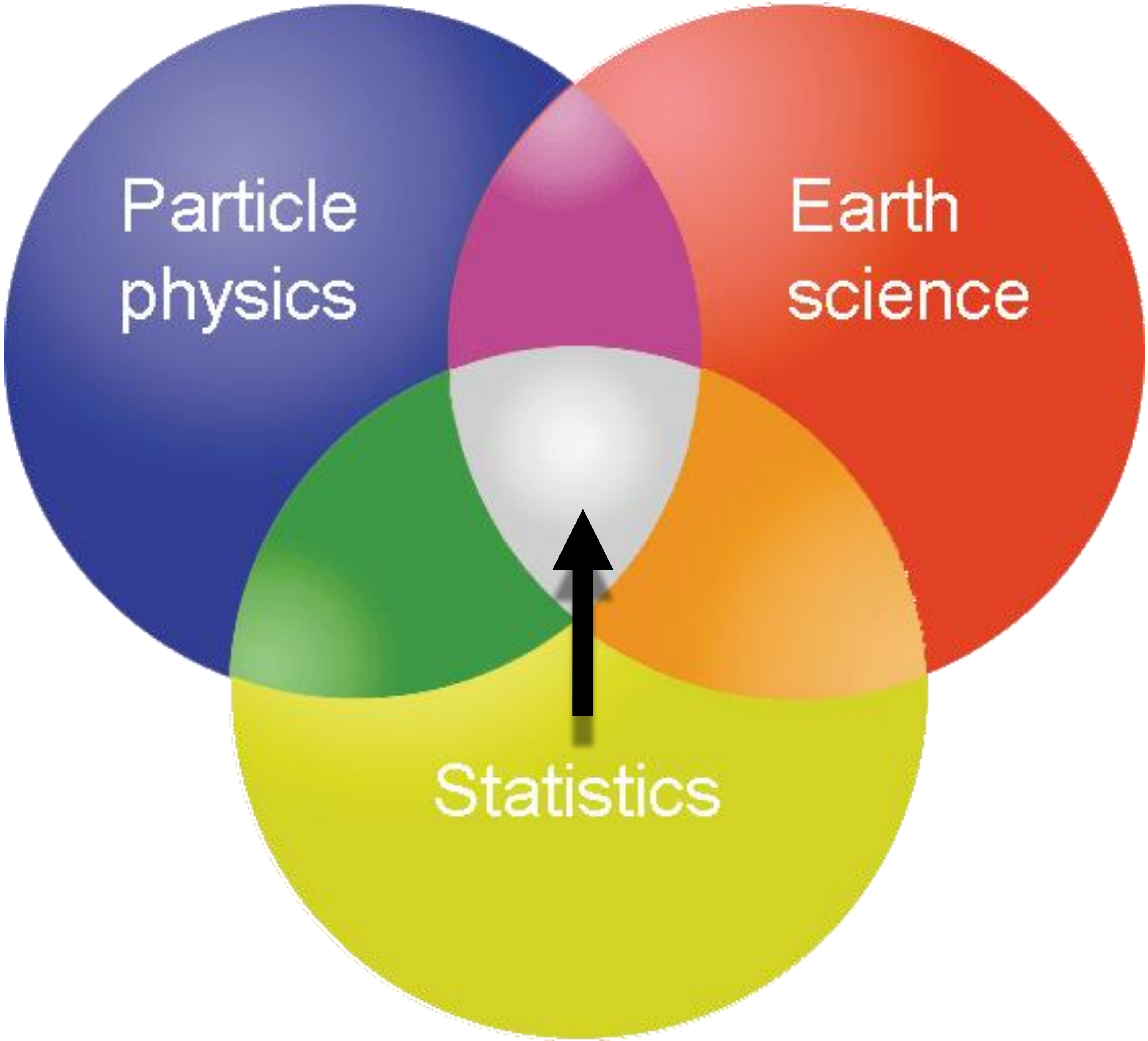
Particle physics
Earth science
Statistics

Radiometric investigation of the rocks of Veneto region

- **Collection of 709 rock samples**: the geological map of Veneto at 1:250000 scale was used as a guide for the sampling.
- **HPGe laboratory measurements (U, Th, K)**
- **Statiscal analysis for a refined radiological characterization of the 41 Cartographic Units**, characterized on the base of their lithologic properties and their stratigraphic relations.

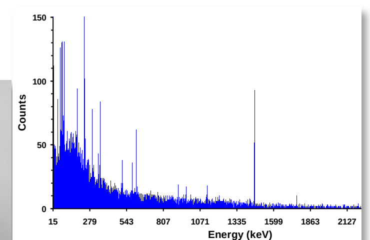

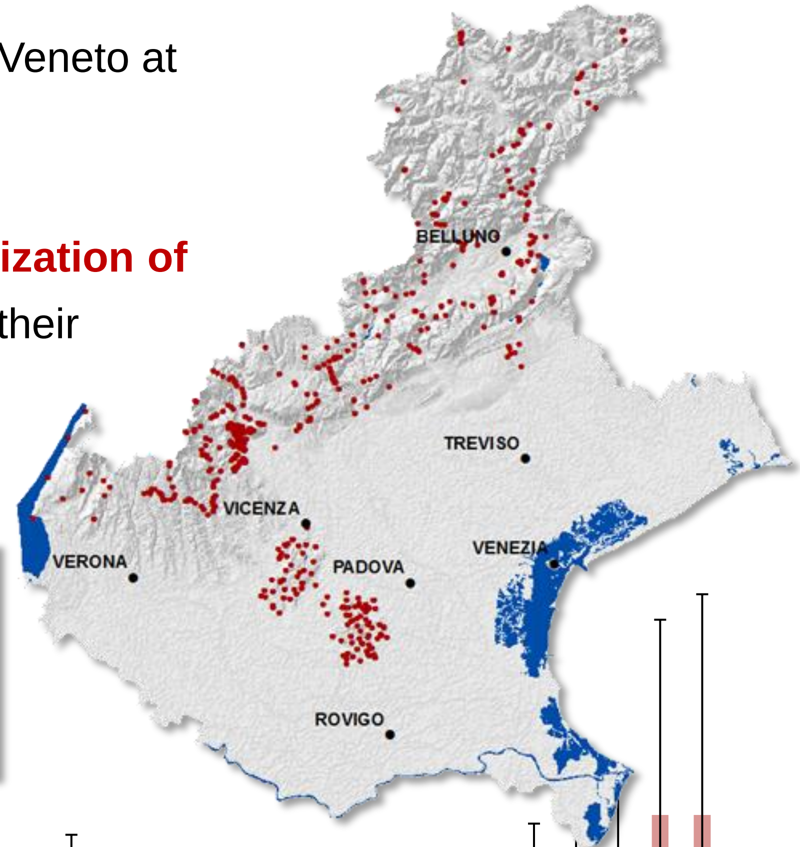

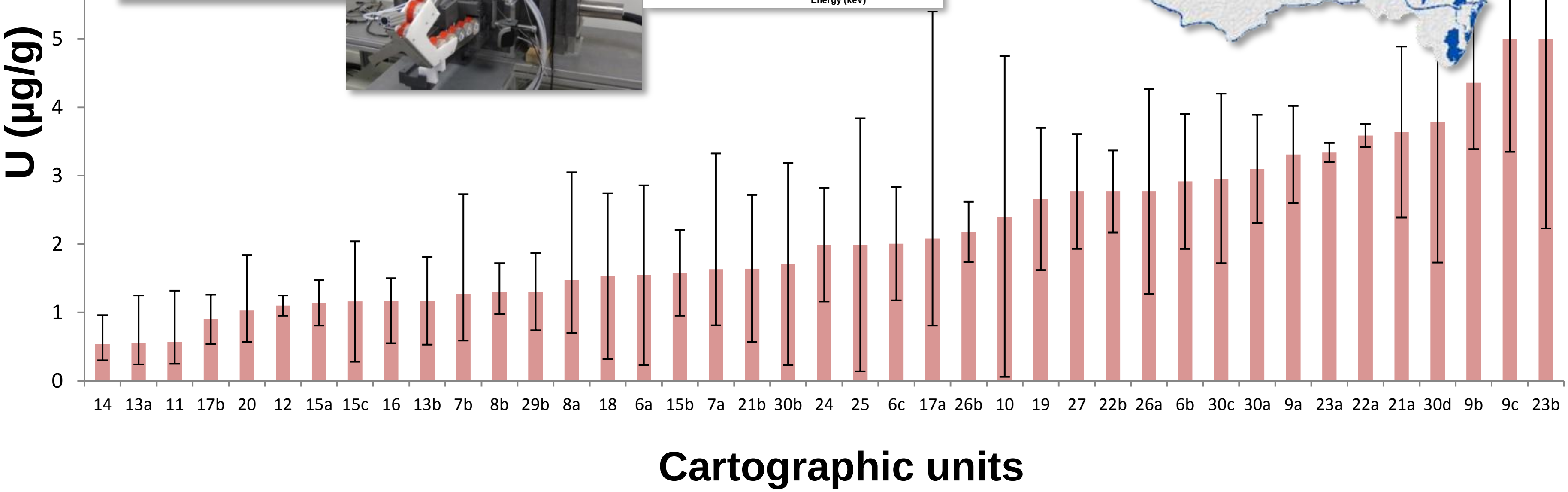

Airborne gamma ray survey of the alluvial plain

- ~19000 points of K, U and Th abundances at ground level
- 12 sec (~ 325 m) of spectral acquisition interval
- each data correspond to an area of 0.6 km^2

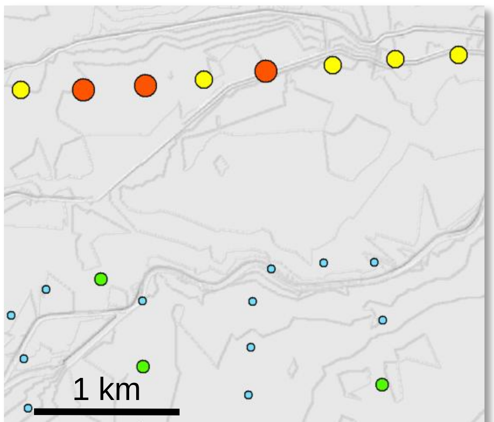

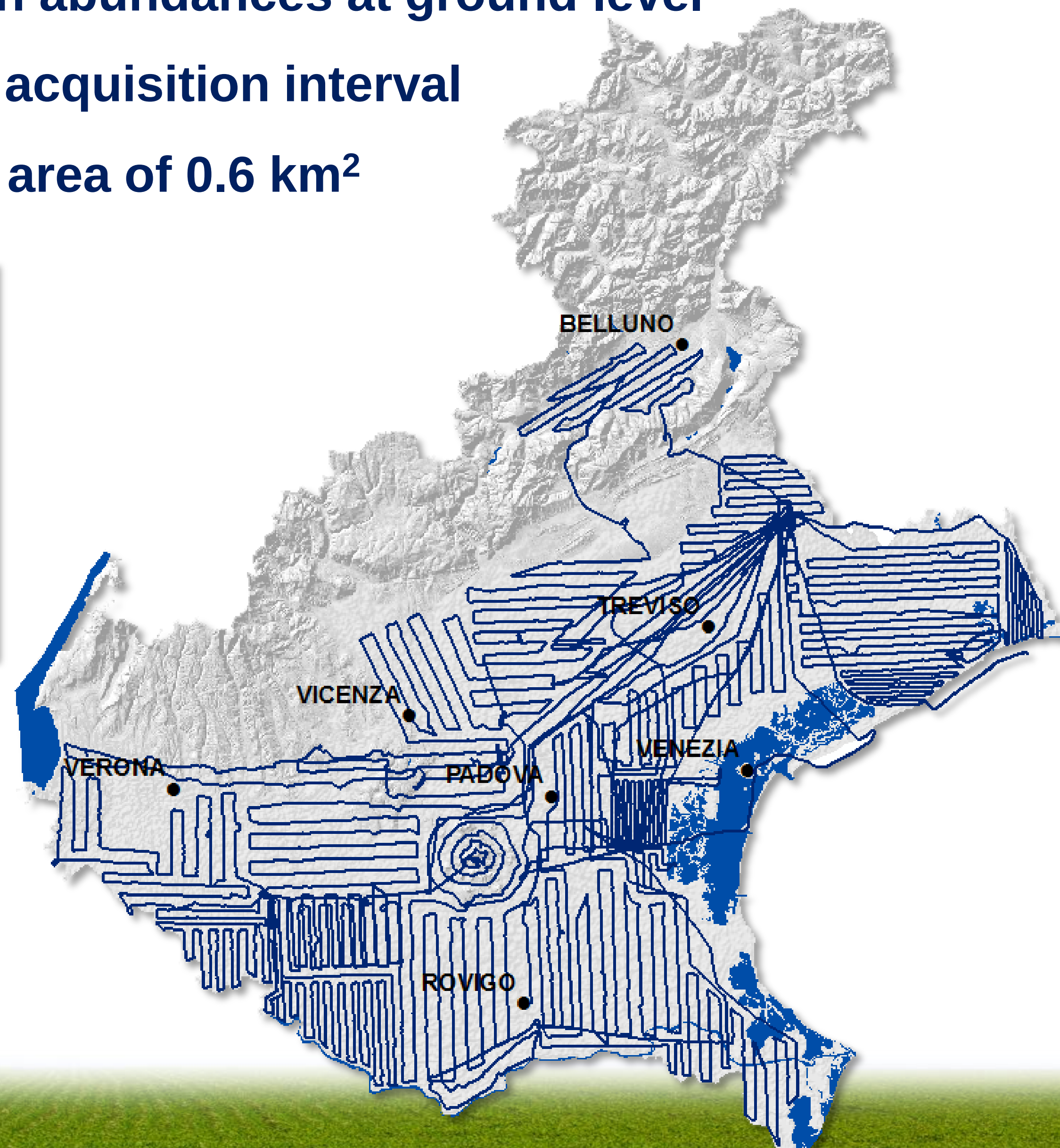

The Ordinary Kriging method

GENERAL ESTIMATOR

$$Z^*(x_0) = \sum_{i=1}^{n} \lambda_i Z(x_i)$$

x_0 = target point

$Z(x_i)$ = measured samples

λ_i = weight assigned to the samples

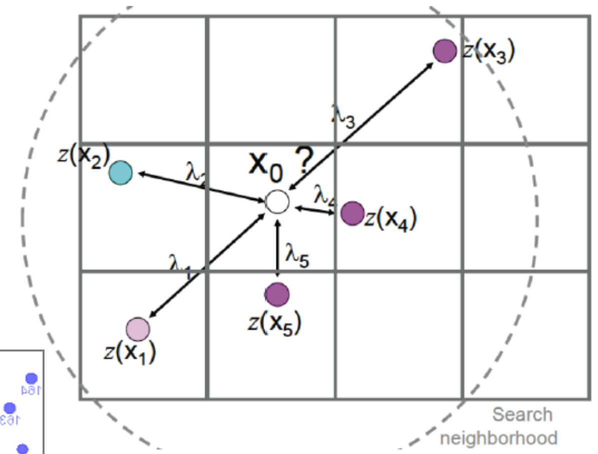

1) Statistical analysis: description of the dataset

2) Study of the spatial variability computation of the Experimental Semi-Variogram (ESV):

$$\gamma(h) = \frac{1}{2m(h)} \sum_{i=1}^{m(h)} \left[Z(x_i + h) - Z(x_i) \right]^2$$

m(h) = number of sample value pairs within distance h

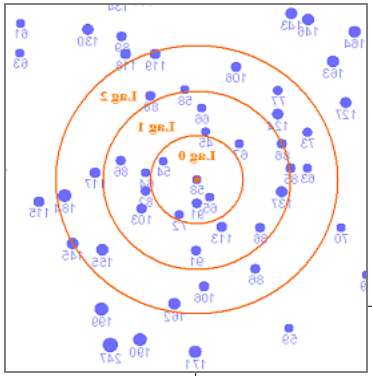

3) Modeling of ESV with a theoretical function (e.g. spherical, exponential, gaussian) describing the real tendency.

4) Cross validation procedure for testing the assumptions of the adopted model.

5) Spatial interpolation: on the base of the ESV model, the values of the variables are estimated together with uncertainties in a GRID with an appropriate spatial resolution

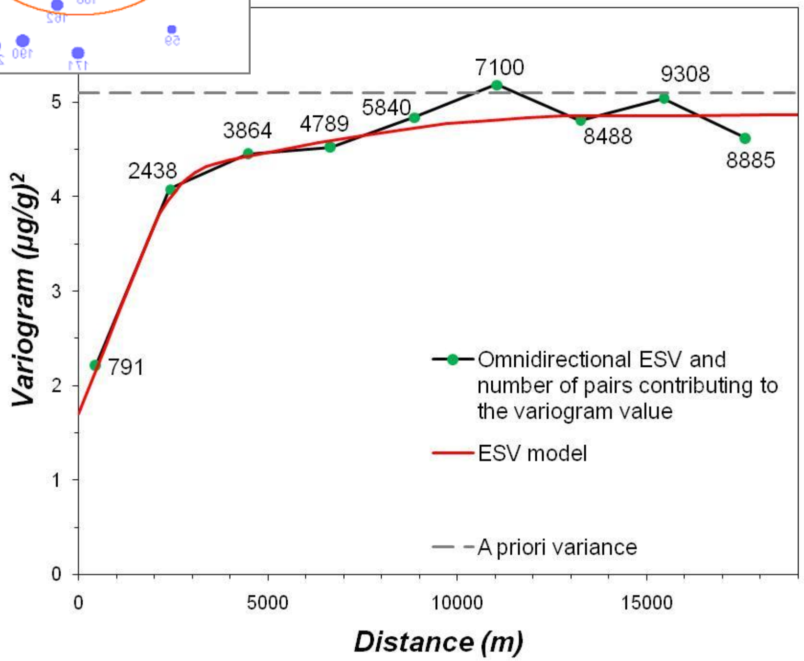

An input dataset with heterogeneous measurement errors

The area (2100 km^2), characterized by several calc-alkaline plutons emplaced within migmatitic massifs and amphibolite-facies metamorphic rocks, is a benchmark for the study of ‘hot’ collisional chains.

Variscan Basement of NE Sardinia

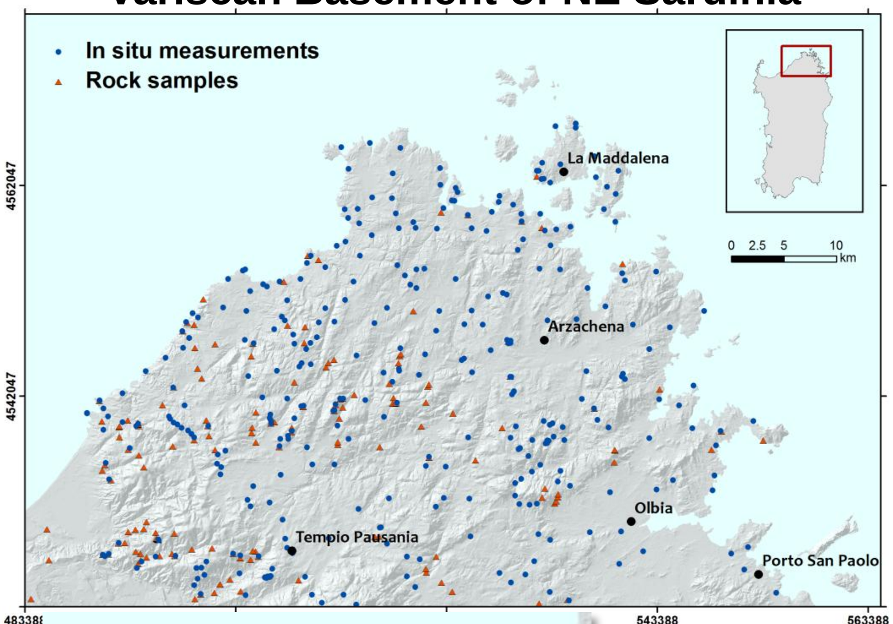

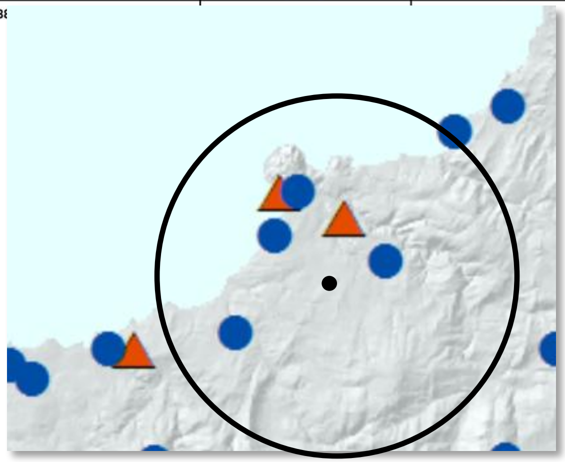

535 input data

167 laboratory measurements (HpGe)

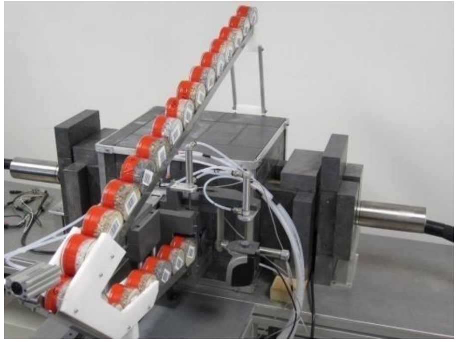

$\sigma_{HpGe}(U) \sim 5\%$

368 ground measurements NaI(Tl)

$\sigma_{NaI}(U) \sim 20\%$

Kriging with Variance of measurement errors

• The **overall uncertainties** of the two different gamma-ray spectrometry techniques are introduced as input.

• During the estimation process difference **weights** are assigned on the base of the **degree of confidence** associated to the measurements

Uranium map of the Variscan Basement of NE Sardinia

INPUT DATA

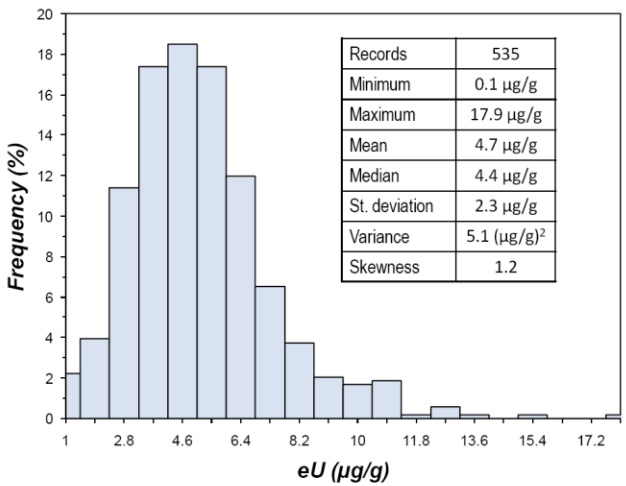

ESV MODEL

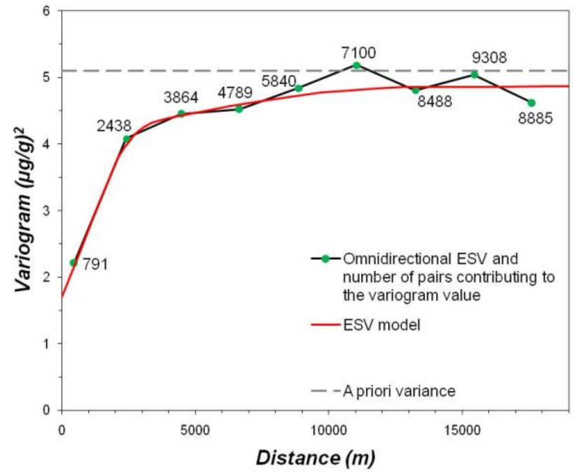

OUTPUT MODEL

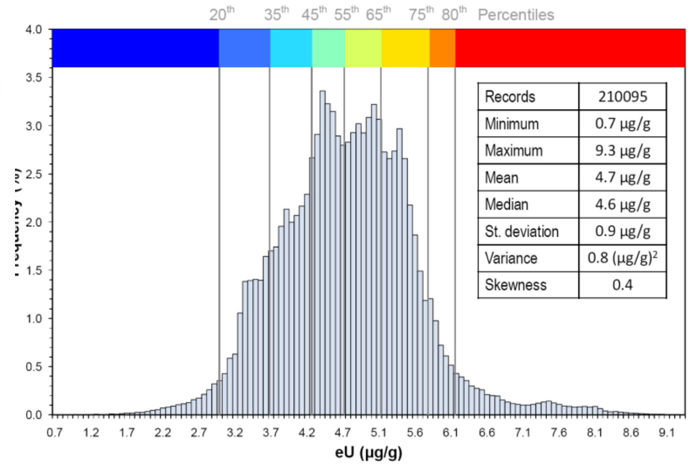

The accuracy of the spatial model in terms of the variance normalized with respect to the estimated values is reported with contour lines in percentage.

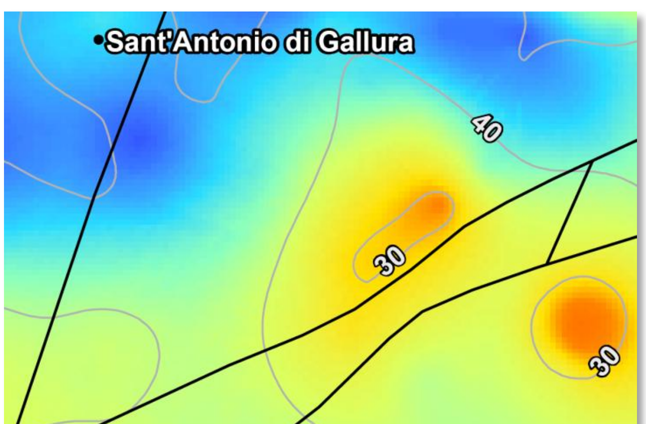

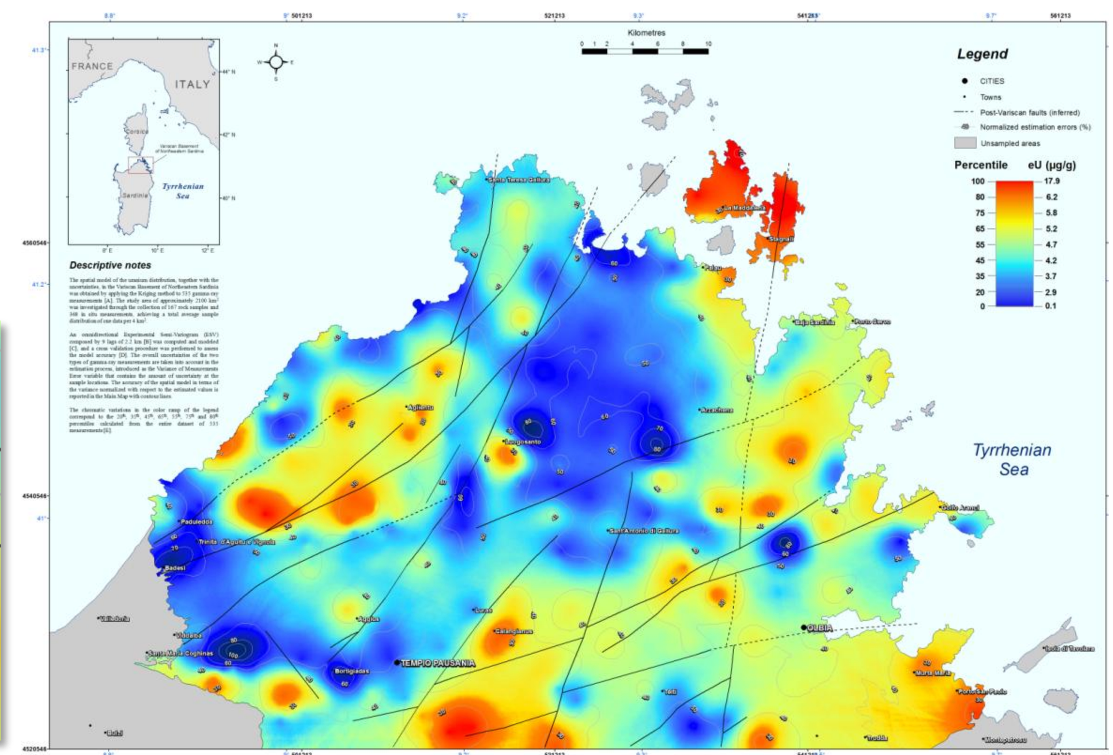

Understanding the evolution of a pluton through U distribution

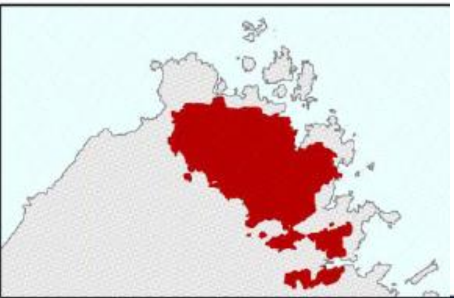

This elongated pluton was emplaced in three concentric granitic shells: in the core are exposed the more mafic terms whereas the external part is composed of felsic rocks, the more evolved magmatic products.

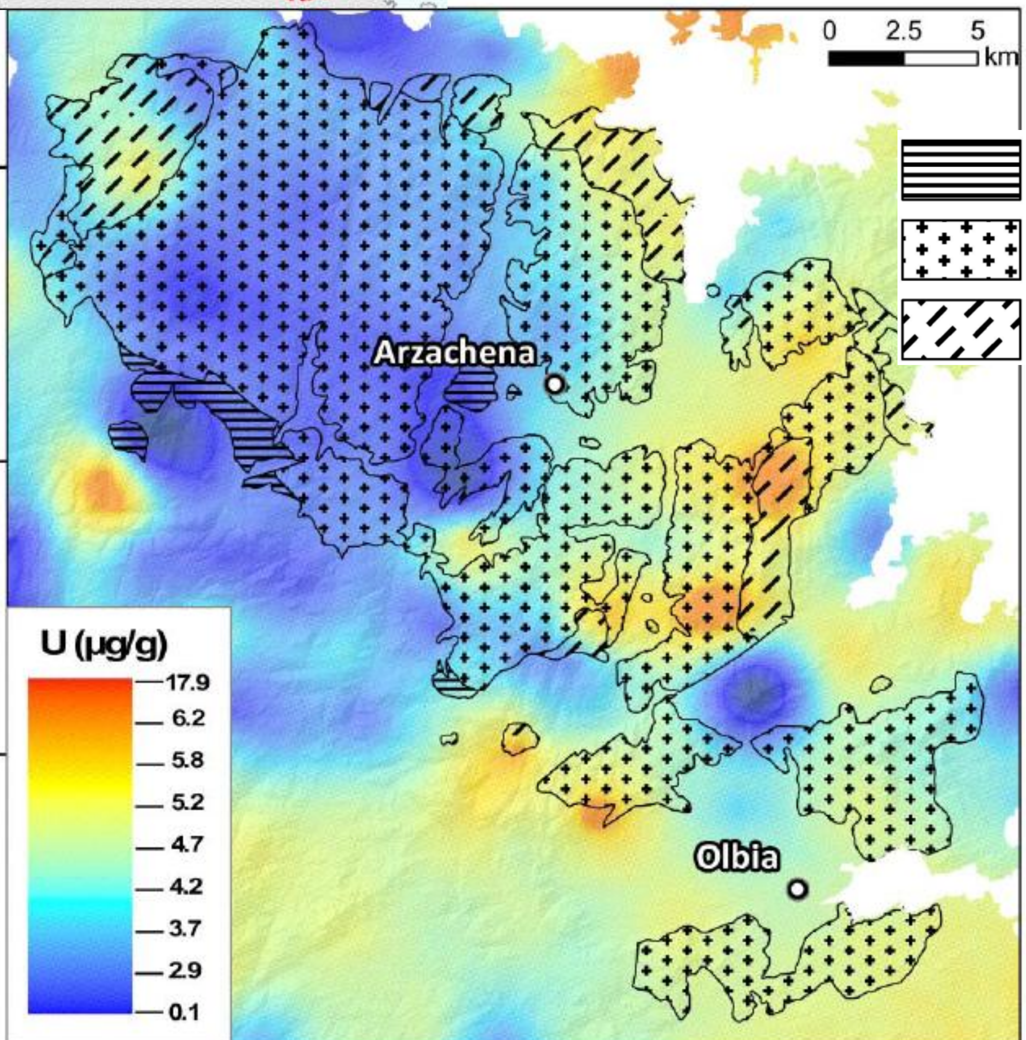

U(µg/g)

	Samples	Model
Granodiorite	2.6 ± 0.6	3.4 ± 0.4
Monzogranite	4.4 ± 1.5	4.3 ± 0.8
Leuco-Monzogranite	6.2 ± 1.9	4.9 ± 0.7

Relevant insights

- Link between U abundances and different petrological associations related to the **magmatic differentiation** during pluton emplacement

- Strong positive correlation between the presence of U-bearing accessory minerals and the **evolution of magmatic systems**.

- Comparison with the proposed **conceptual model** of the pluton emplacement.

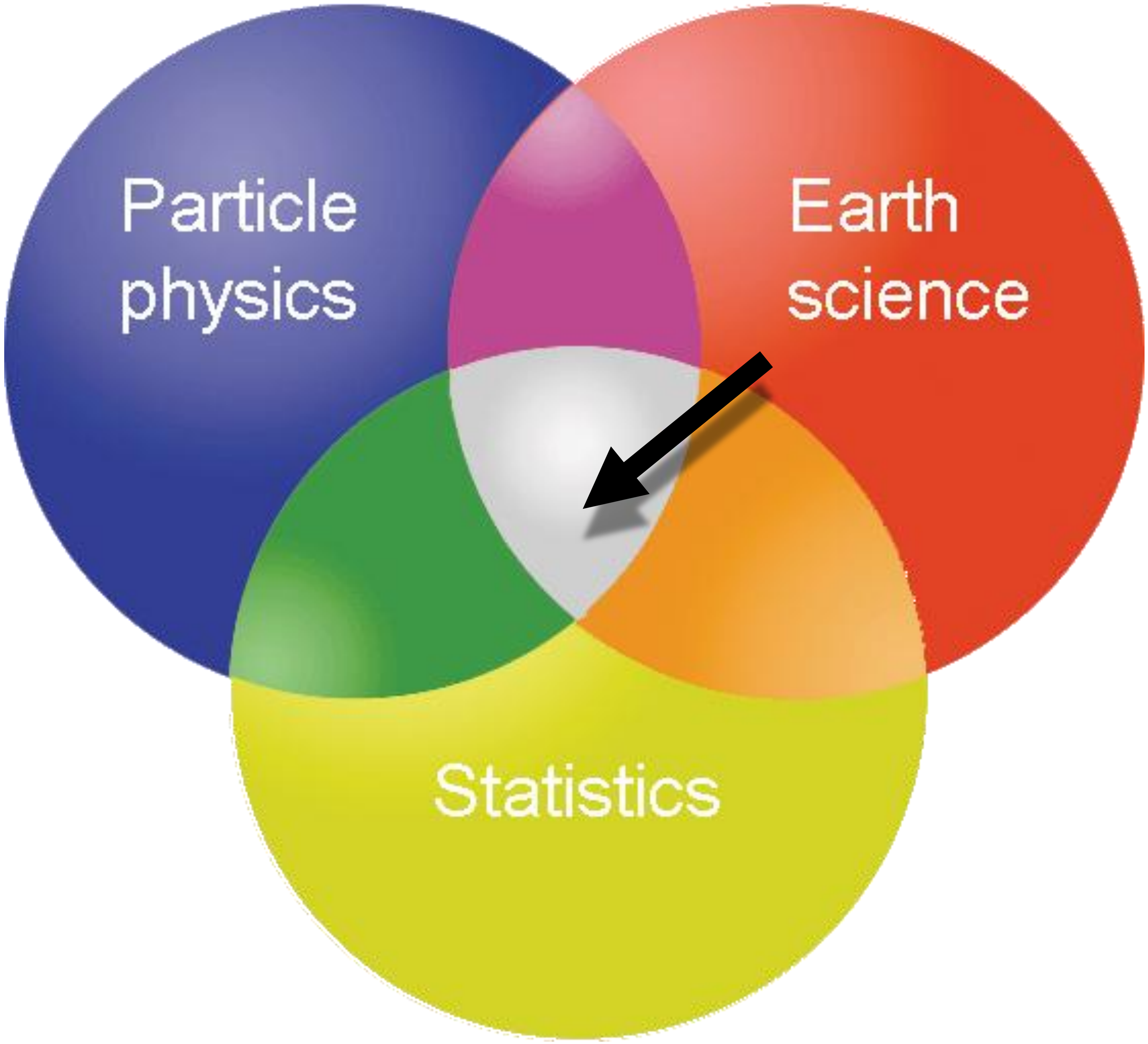

Particle physics
Earth science
Statistics

A multivariate spatial interpolation of γ-ray data

Elba Island (Tuscany)

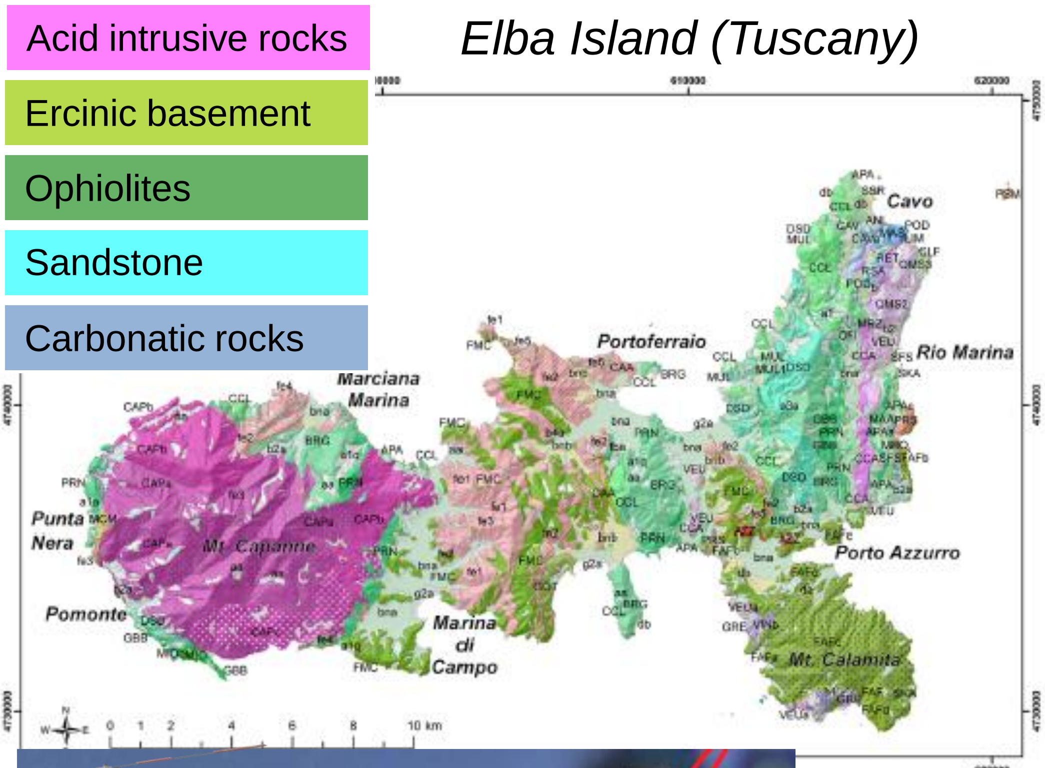

COLLOCATED COKRIGING

- **Primary variable**: abundances of K, eU, or eTh measured via airborne γ-ray spectrometry.
- **Secondary variable:** the geological map at 1:10000 scale with 73 geological formations reporting lithologic details.

PROCEDURE

Step 1 - Creation of a CONTINUOS GRID: for each of the 73 geological formation a progressive number is assigned .

Step 2 - The AIRBORNE γ-RAY measurements are spatially conjoined to the geological grid.

Step 3 - A MULTIVARIATE point dataset is obtained for spatial interpolation.

The Experimental Cross-Variogram

The spatial variability is studied by computing and modeling also the Cross Experimental Semi-Variogram (X-ESV):

$$\gamma(h) = \frac{1}{2m(h)} \sum_{i=1}^{m(h)} \left\{ \left[Z_1(x_i) - Z_1(x_i + h) \right] \left[Z_2(x_i) - Z_2(x_i + h) \right] \right\}$$

ESV – Primary variable

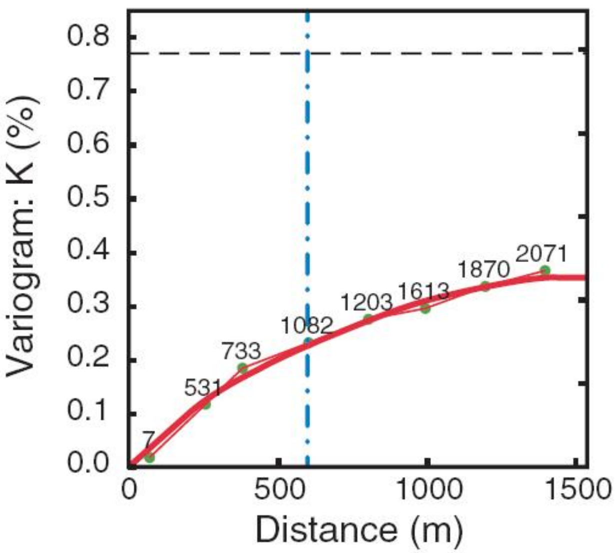

ESV – Secondary variable

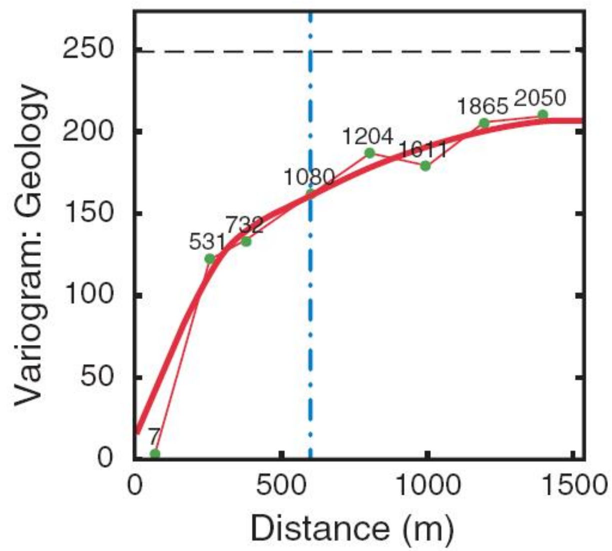

X-ESV

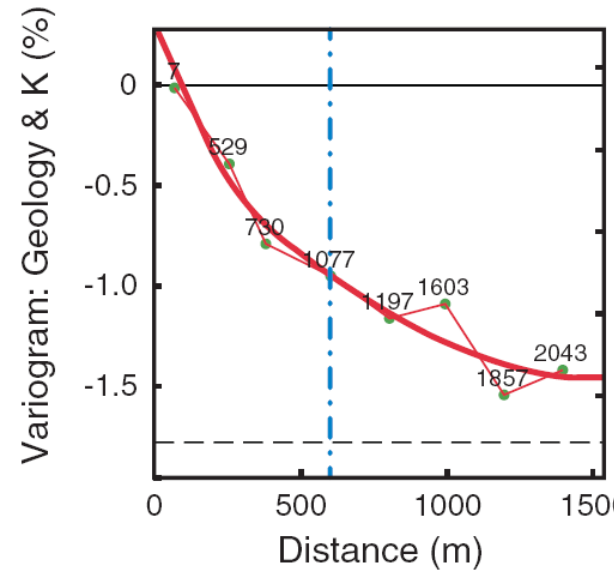

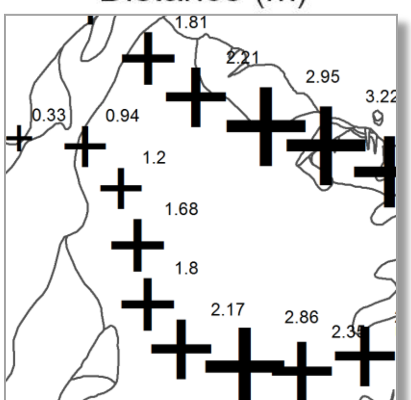

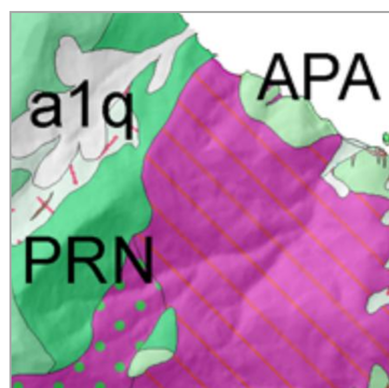

This geostatistical tool gives value to the information of the geological map, enhancing the predictions.

Map of K distribution of Elba's Island

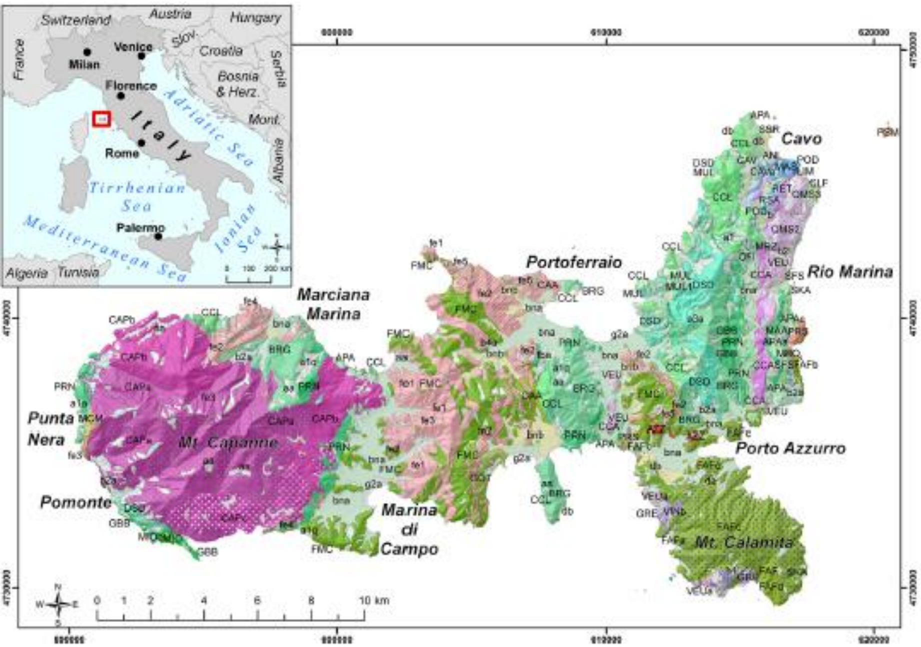

Although a unique number to each geological formation is assigned, the internal variability of the radiometric data is not biased by the multivariate interpolation

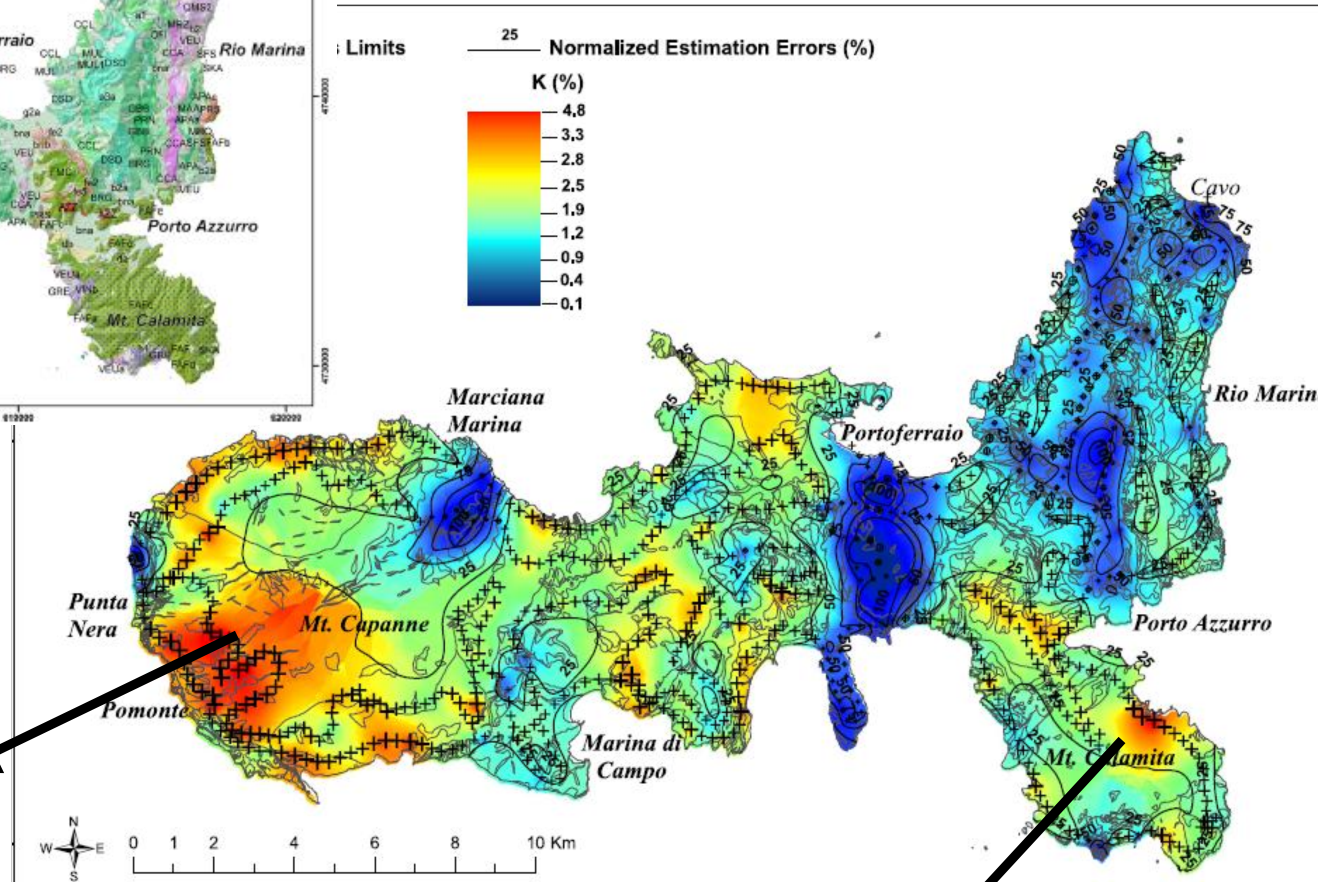

The distribution of K in the Mt.Capanne granitic complex reflects the variability of **K-feldaspar megacryst** content. and can be also related to an important **tectonic lineament** recognized in this area.

Anomaly of **high K abundance**: the radiometric survey identified the presence of **felsic dykes** not reported in the geological map but confirmed by recent studies.

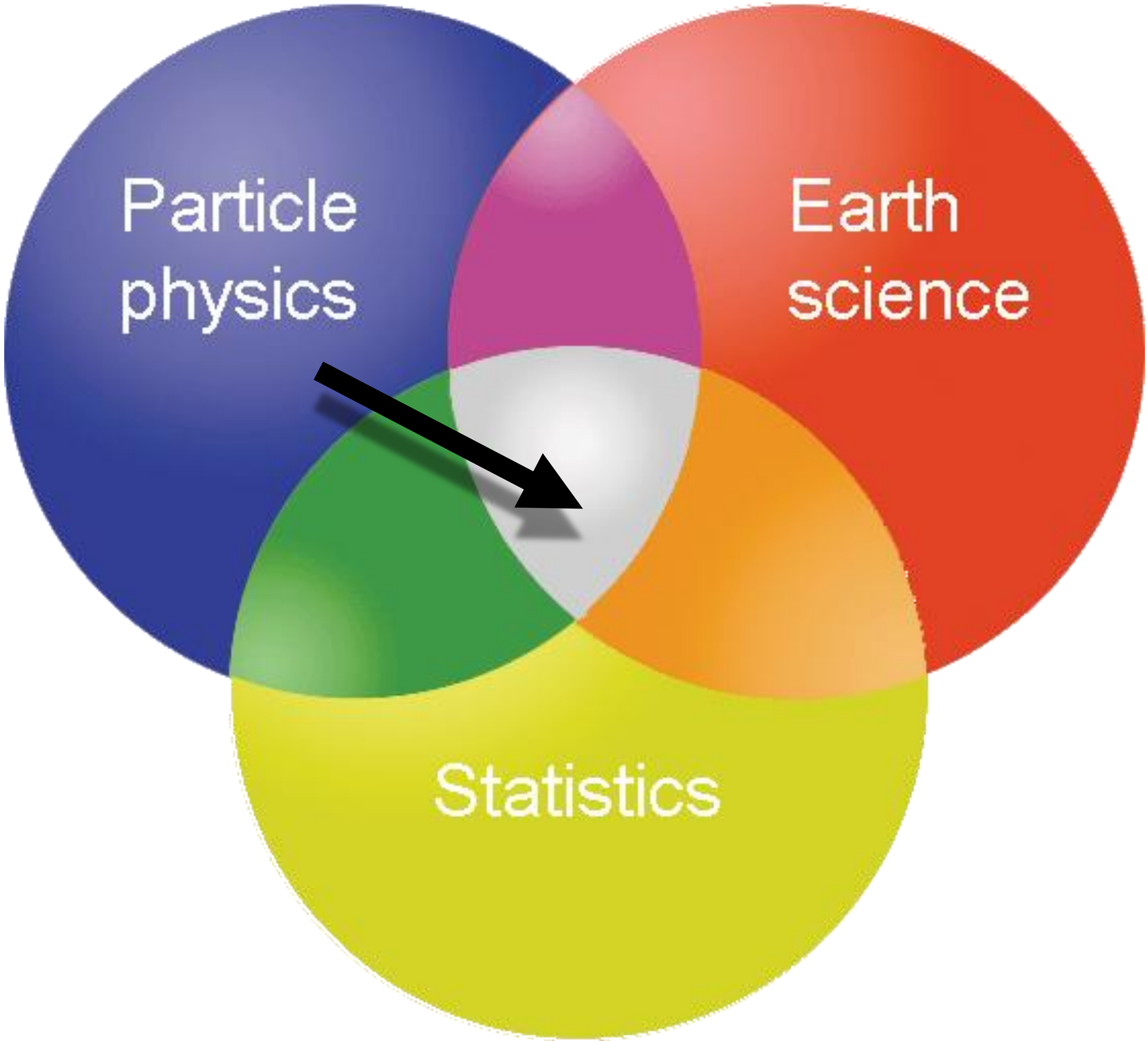
Particle physics
Earth science
Statistics

Calculation of geoneutrino signal

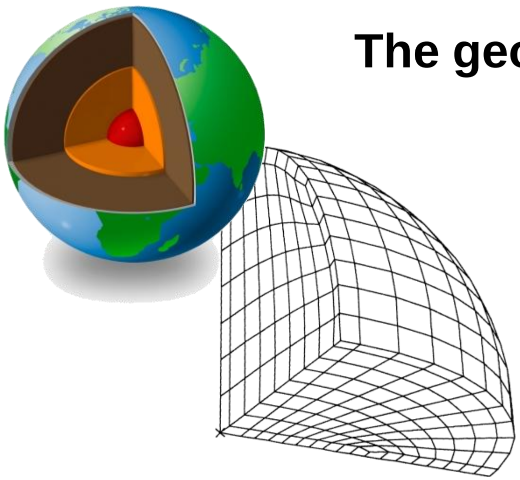

The geoneutrino flux produced by the element X, i.e. U and Th, is:

Geoeneutrino production rate

Density of the voxel

Elemental mass abundance of X in the voxel

$$\phi(X) = \frac{\varepsilon_{\bar{\nu}_X}}{4\pi} \int_V \frac{\rho(\vec{r}')\, a_X(\vec{r}')}{\left|\vec{R} - \vec{r}'\right|^2} dr'$$

Distance between the detector and the centre of the voxel.

The **oscillated geoneutrino flux** is calculated by taking into account three flavor survival probability $\mathbf{P_{ee}}$ and the geoneutrino energy spectrum:

$$P_{ee}(E_{\bar{\nu}_e}, \vec{r}) = \cos^4(\theta_{13}) \left(1 - \sin^2(2\theta_{12}) \sin^2\left(\frac{\delta m^2 \vec{r}}{4E_{\bar{\nu}_e}} \right) \right) + \sin^4(\theta_{13})$$

Assuming the detector efficiency **ε = 1** and 10^{32} free target protons $\mathbf{N_p}$. the geoneutrino signal in **TNU** originated by the radionuclide **X** for a fixed distance **r**, can be calculated:

$$S(\vec{r}, X) = \phi(\vec{r}, X) P_{ee}(\vec{r}, X) \langle \sigma \rangle_X$$

Integrated inverse beta reaction cross section

[1 TNU = 1 event per 10^{32} free proton per year]

Detecting geoneutrinos around the world

In one site, for each radioisotope (^{238}U, ^{232}Th) the expected geo-neutrino signal is the sum of three contributions:

$$S_{EXP} = S_{LOC} + S_{FFC} + S_{M}$$

$$S_{Mantle} = S_{Measured} - (S_{LOCal} + S_{Rest\ Of\ Crust})$$

EXP = total expected signal
LOC = crust of the region within some hundreds km from the detector
FFC = Far Field Crust
M = mantle signal

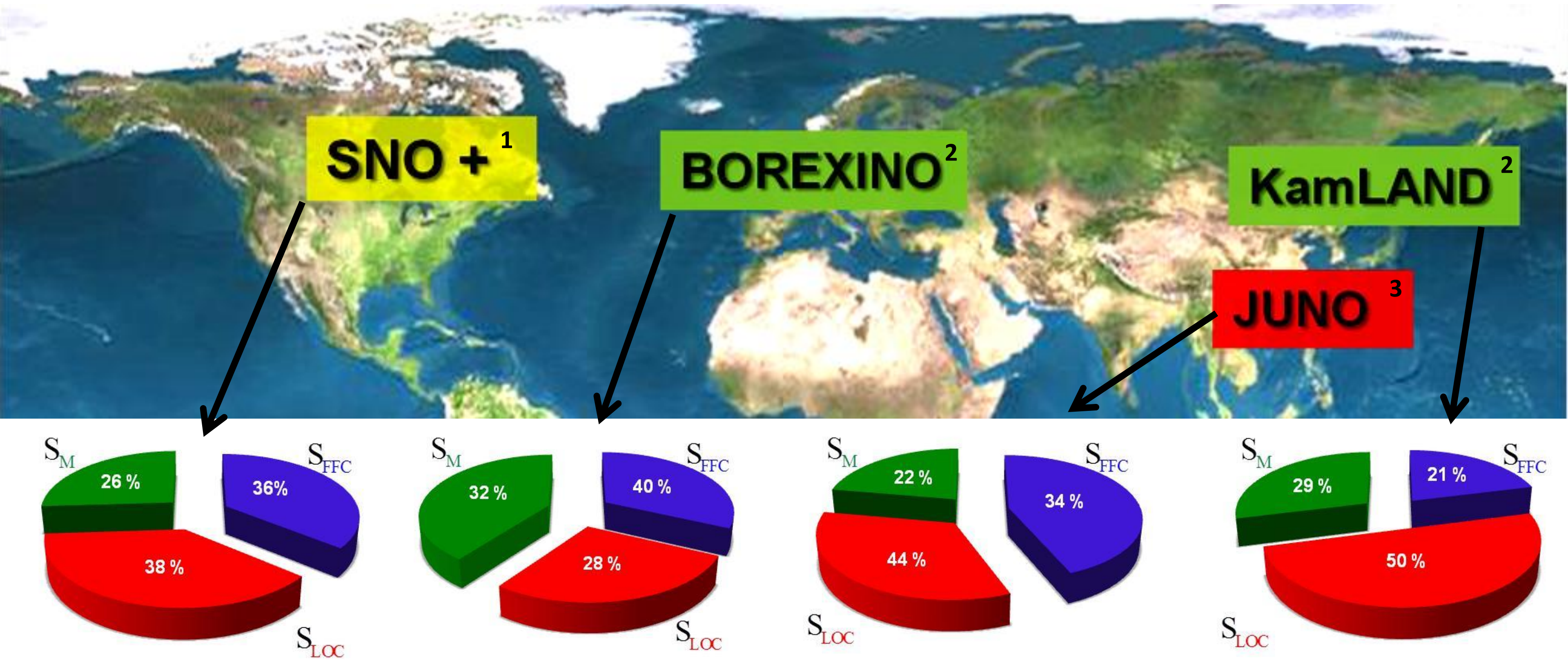

1 – Huang et al. 2014, Geochemistry, Geophysics, Geosystems 15(10).
2 - Fiorentini et al 2012 , Physical Review D 86(3) 3 - Strati et al. 2015 , Progress in Earth and Planetary Science 2(1).

Modeling the geoneutrino flux

$$S(\vec{r}, X) = \phi(\vec{r}, X)\, P_{ee}(\vec{r}, X) \langle \sigma \rangle_X$$

$$\phi(X) = \frac{\varepsilon_{\bar{\nu}_X}}{4\pi} \int_V \frac{\rho(\vec{r}\,')\, a_X(\vec{r}\,')}{\left|\vec{R} - \vec{r}\,'\right|^2} dr'$$

UC

U and Th content measured in representative samples

Literature data, geological maps and interpreted seismic profiles

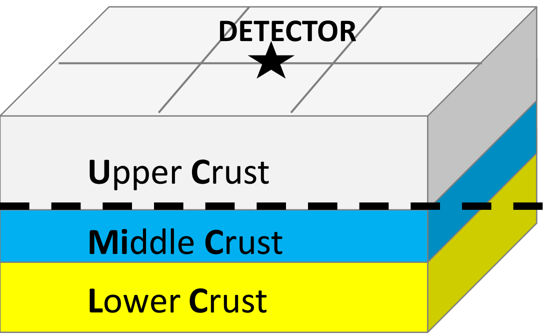

$$\Phi(a\,;\, \rho\,;\, dV)$$

MC

LC

U and Th abundances inferred from seismic arguments

Estimations from seismic velocities and other geophysical data

"Geochemical uncertainties" ~ 15%

Geophysical uncertainties ~ 5%

A crustal 3D model surrounding SNO+

- **SNO+** is a 1kton LS detector located in Ontario (Canada) in the Superior Province, one of the world's largest Archean cratons

- We modeled the crust of the six 2° x 2° crustal tiles (**440 km x 460 km)** for predicting geoneutrino signal

- The goal was to define the geometry of **LC, MC** and 7 main reservoirs of the **UC**, assigning them U and Th abundances

- We digitized **velocity contours** (6.6, 6.8 and 8.0 km/s) in order to extract **depth** of the top of MC (TMC), LC (TLC) and Moho Discontinuity (MD)

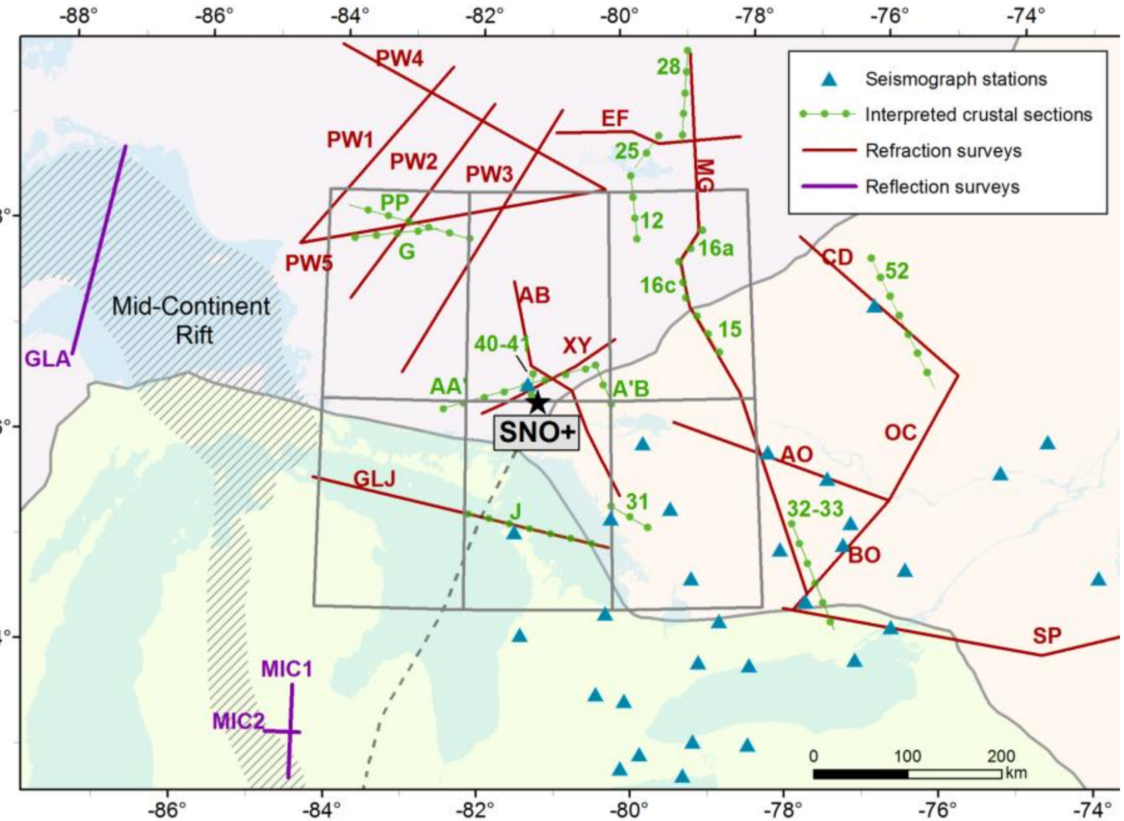

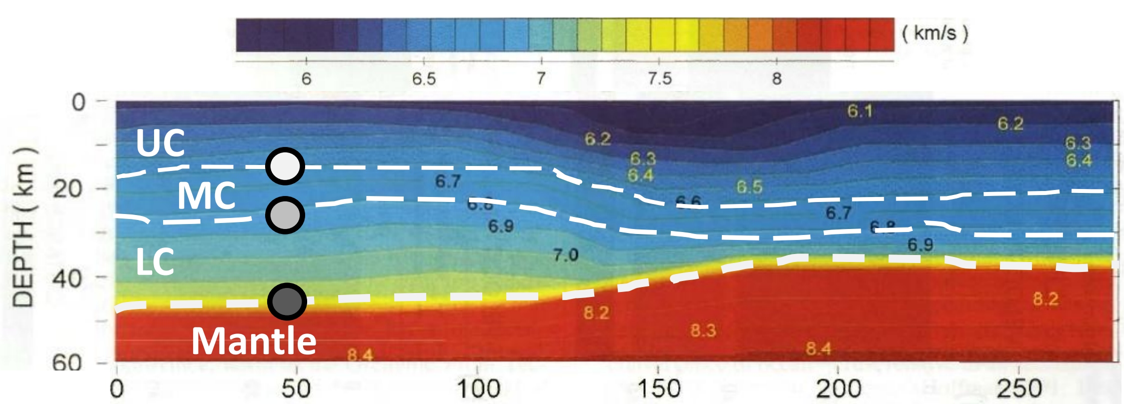

Latitude	Longitude	Depth
46.85 °	- 81.78 °	18.4 km
46.85 °	- 81.78 °	27.7 km
46.85 °	- 81.78 °	47.6 km

Modeling the geophysical discontinuities surfaces

Input

Depth-controlling points obtained by 15 refraction lines, 3 reflection lines and data from 32 seismographic stations

	N° points
Top of MC (TMC)	343
Top of LC (TLC)	343
Moho discontinuty (MD)	392

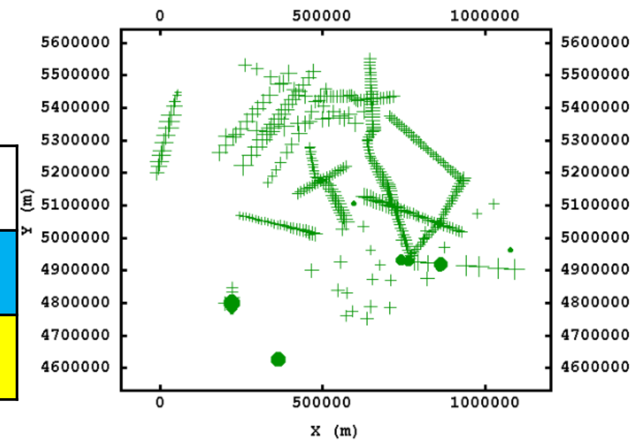

ORDINARY KRIGING: the value of the depth in **unobserved locations** is estimated from **input data points** taking into account the **spatial continuity** of the variables.

Output

•Estimated maps of TMC, TLC and MD depth with a 1 km × 1 km resolution.

• Maps provides the Normalized Estimation Errors (NEE).

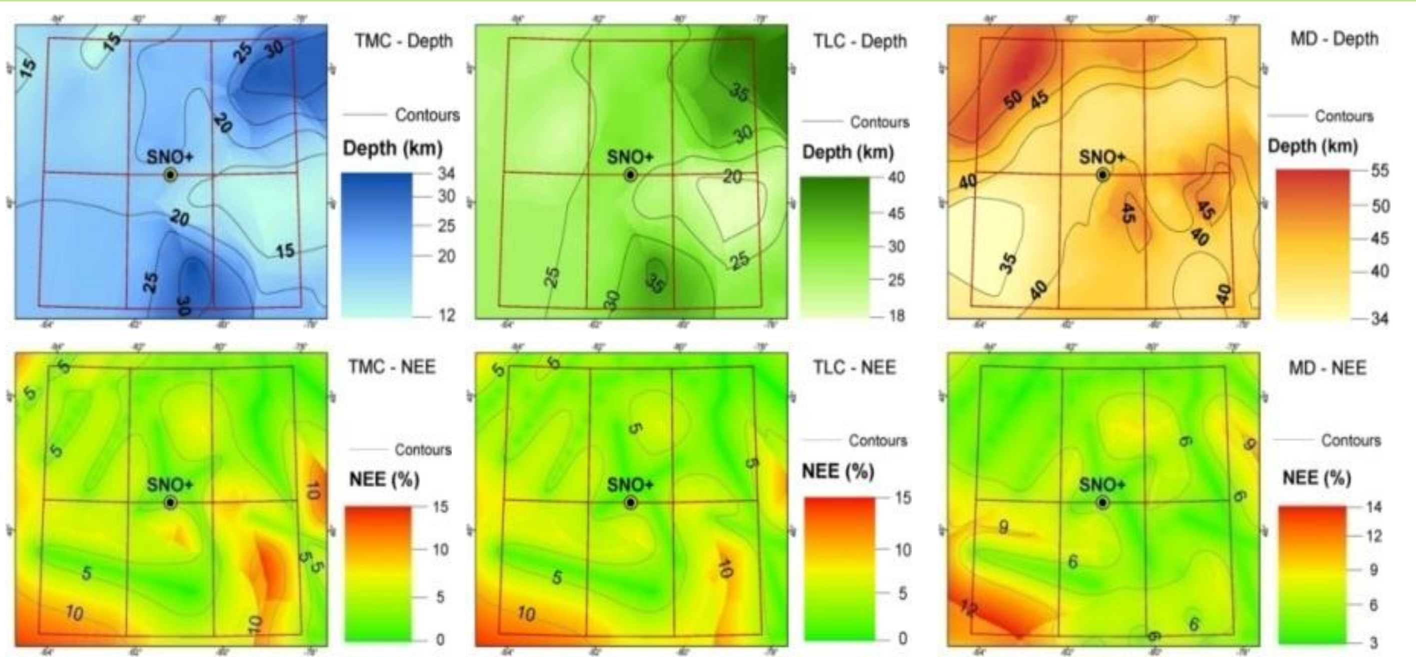

The geophysical uncertainties at SNO+

• For the first time the **masses** of the main crustal reservoirs containing U and Th are estimated together with their uncertainties in the region surrounding SNO+.

	CRUST 1.0*	Huang et al. 2014		
	M [10^{18} kg]	Volume [10^{6} km^{3}]	ρ [g/cm^{3}]	M [10^{18} kg]
UC	**6.6**	4.2 ± 0.2	2.73 ± 0.08	**11.5 ± 0.6**
MC	**8.1**	1.3 ± 0.1	2.96 ± 0.03	**3.8 ± 0.3**
LC	**8.0**	3.2 ± 0.2	3.08 ± 0.06	**9.9 ± 0.6**
Total	**22.7**	8.7 ± 0.5	-	**25.2 ± 1.6**

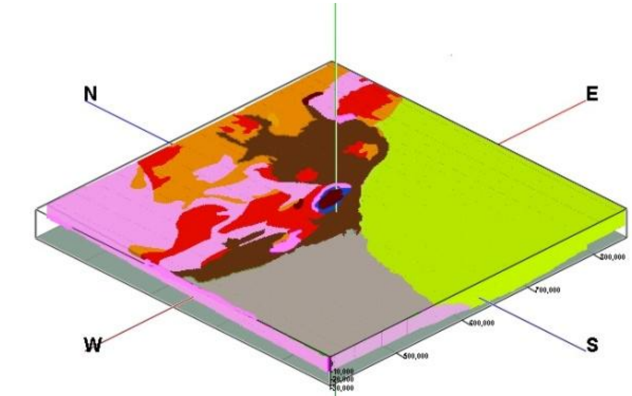

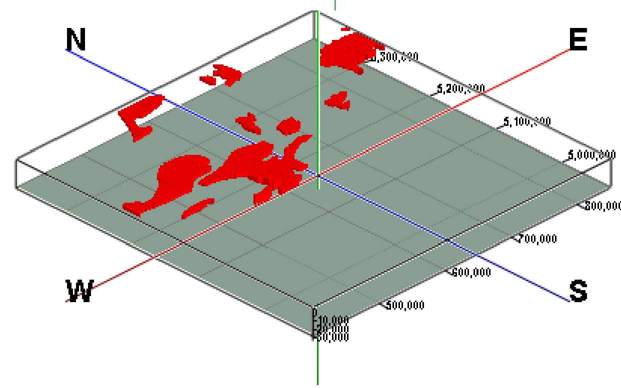

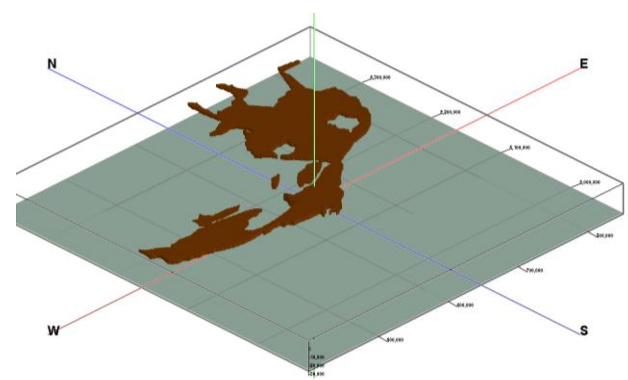

• The relative uncertainties of the reservoirs masses are of ~ 6%.

• Together with uncertainties of U and Th abundances these results are crucial for a reliable estimation of geoneutrino signal in SNO+.

* Laske et al. [2013] at **http://igppweb.ucsd.edu/~gabi/rem.html**

Geoneutrino signal at SNO+ from the local crust

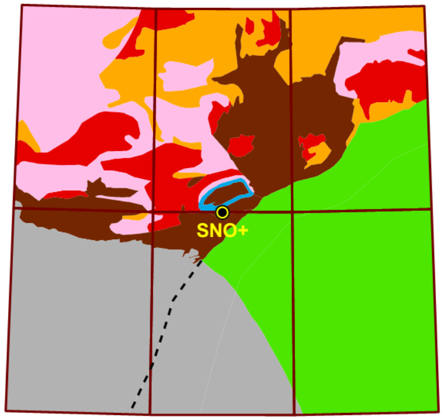

- After the refinement, the regional geoneutrino signal expected at SNO+ decreases from **18.9** $^{+3.5}_{-3.3}$ TNU (Huang et al. 2013) to **15.6** $^{+5.3}_{-3.4}$ TNU (Huang et al. 2014).
- The **Huronian Supergroup** is predicted to be the dominant source of the geoneutrino signal and the primary source of the large uncertainty on the local predicted geoneutrino signal.

Lithologic unit of UC	Vol. (%)	U (ppm)	Th (ppm)	S(U+Th) [TNU]
Tonalite/Tonalite gneiss (Wawa-Abitibi)	60.6	$0.7^{+0.5}_{-0.3}$	$3.1^{+2.3}_{-1.3}$	$2.2^{+1.4}_{-0.9}$
Central Gneiss Belt (Grenville Province)	30.2	$2.6^{+0.4}_{-0.4}$	$5.1^{+6.0}_{-2.8}$	$2.1^{+0.4}_{-0.3}$
(Meta)volcanic rocks (Abitibi sub-province)	2.9	$0.4^{+0.4}_{-0.2}$	$1.3^{+1.2}_{-0.6}$	$0.02^{+0.01}_{-0.01}$
Paleozoic sediments (Great Lakes)	1.3	$2.5^{+2.0}_{-1.1}$	$4.4^{+1.6}_{-1.2}$	$0.05^{+0.04}_{-0.02}$
Granite or granodiorite (Wawa-Abitibi)	2.2	$2.9^{+1.6}_{-1.0}$	$19.9^{+8.4}_{-6.0}$	$0.5^{+0.2}_{-0.1}$
Huronian Supergroup, Sudbury Basin	2.7	$4.2^{+2.9}_{-1.7}$	$11.1^{+8.2}_{-4.8}$	$7.3^{+5.0}_{-3.0}$
Sudbury Igneous Complex	0.1	$2.3^{+0.2}_{-0.2}$	$10.6^{+0.7}_{-0.7}$	$0.8^{+0.1}_{-0.1}$

2014
- *First refined model*

Nov 2015
- Refined characterization of the unit
- Planning of the sampling

May 2016
- *Sampling of the HS unit*
- *Measurements with HPGe detectors.*

2017
- *New refined model*
- *Start of data taking at SNO+*

The goal of JUNO: determination of mass hierarchy but not only…

JUNO is a challenging experiment for measuring directly the mass hierarchy of antineutrinos.

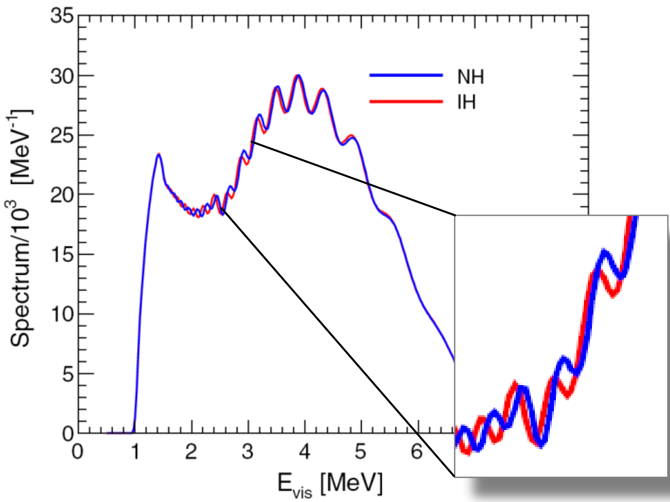

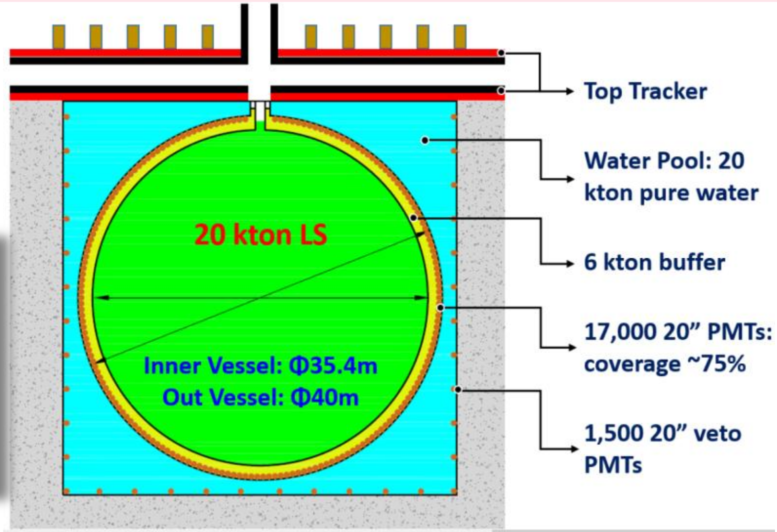

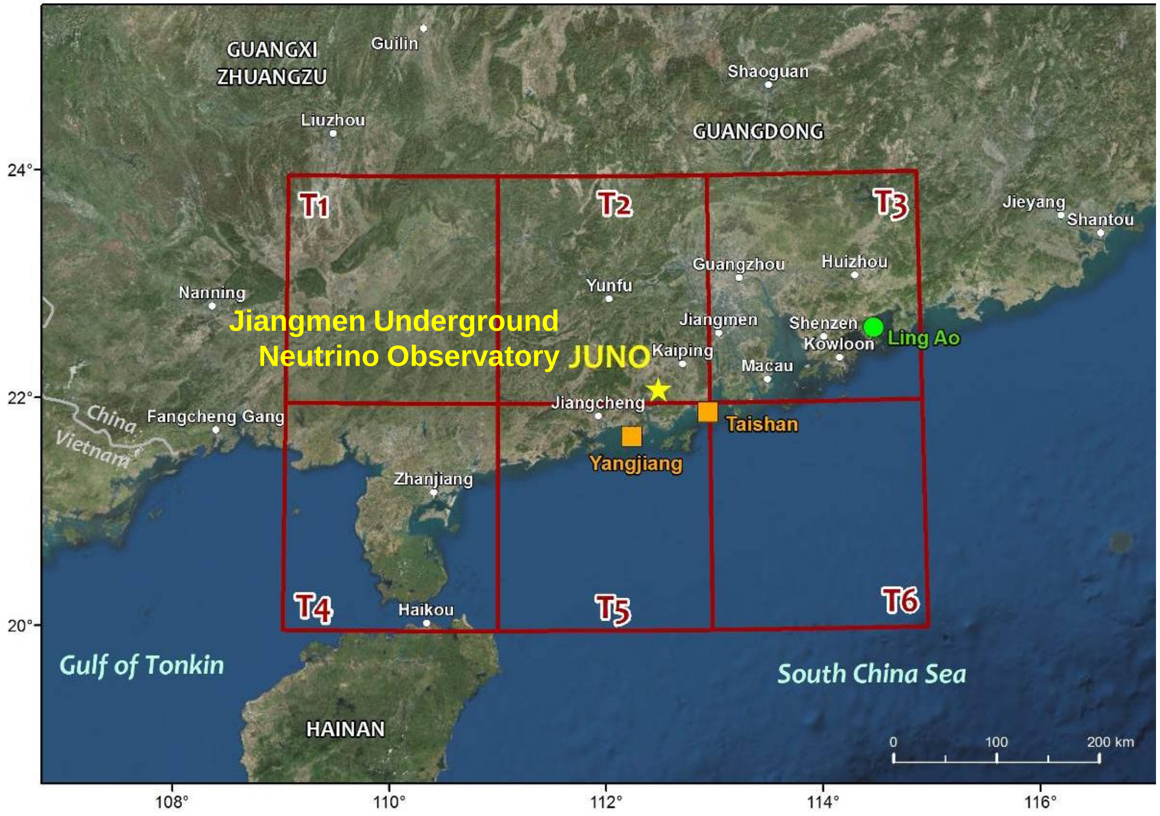

Other scientific goals

- Neutrino oscillation parameters
- Solar neutrinos
- Supernovae neutrinos
- Atmospheric neutrinos
- **Geoneutrinos**

The biggest detector in the world: we expect 408 events/year (to compare with 12 event/year of KamLAND)

Geoneutrino signal contribution

• The **50%** of the total signal comes from the regional crust that lies within **550 km** of the detector.

• The **CRUST** contributes for the **~ 70%** of the total geoneutrino signal.

• At a distance of **100 km,** the crust contribution can be considered the only one (**~30%)**.

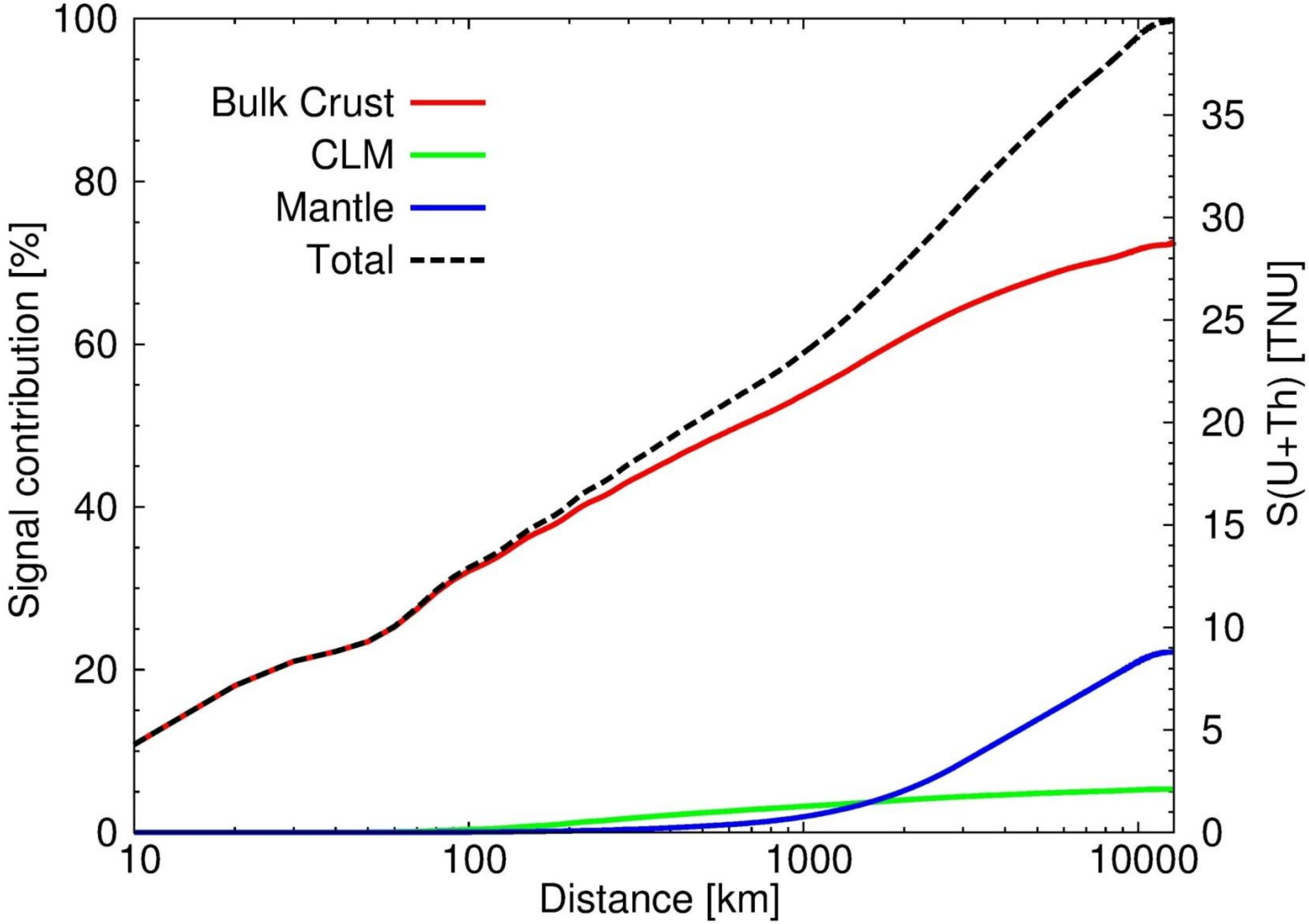

Antineutrino spectra at JUNO

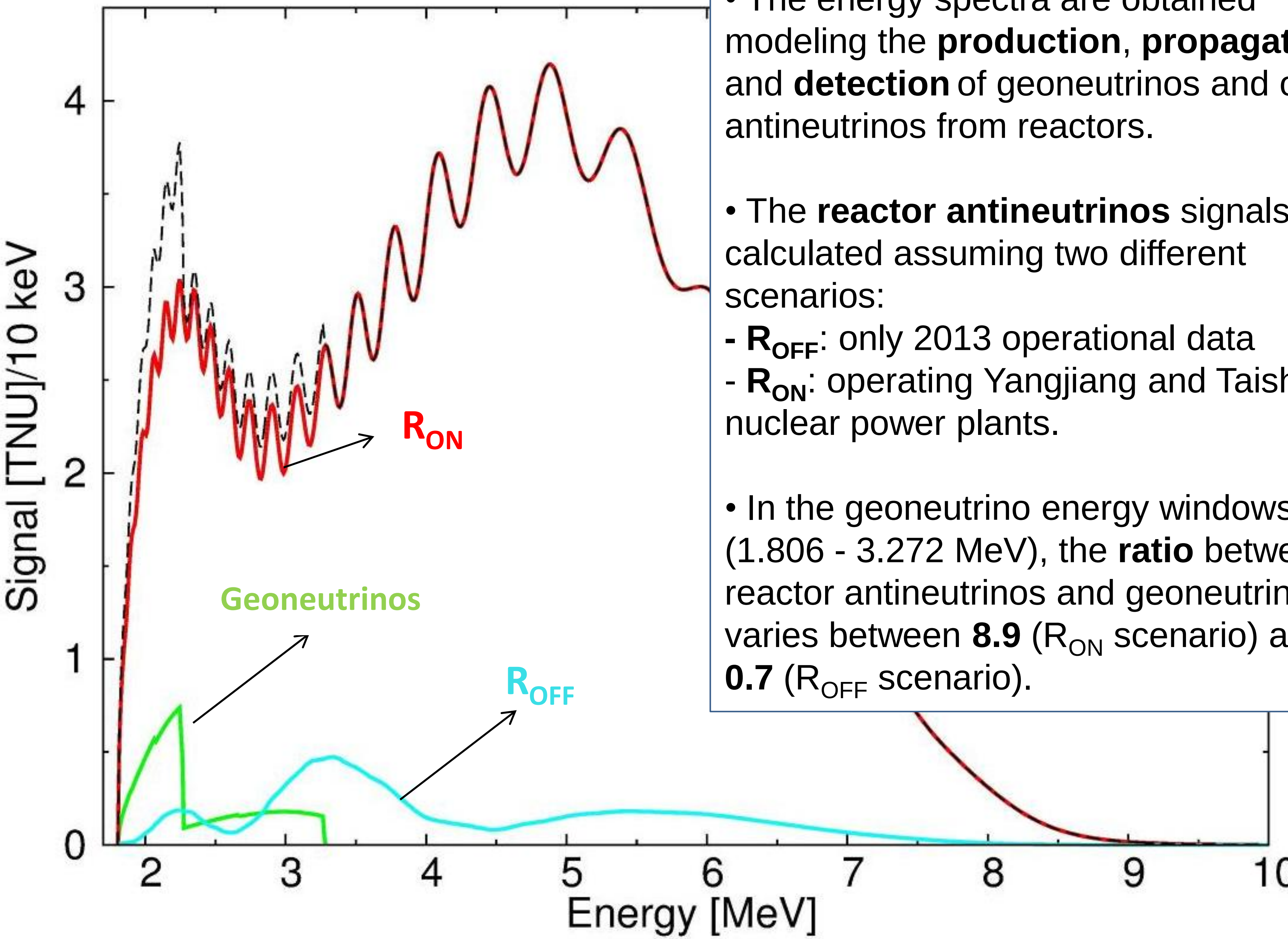

• The energy spectra are obtained modeling the **production**, **propagation** and **detection** of geoneutrinos and of antineutrinos from reactors.

• The **reactor antineutrinos** signals are calculated assuming two different scenarios:
- **R_{OFF}**: only 2013 operational data
- **R_{ON}**: operating Yangjiang and Taishan nuclear power plants.

• In the geoneutrino energy windows (1.806 - 3.272 MeV), the **ratio** between reactor antineutrinos and geoneutrinos varies between **8.9** (R_{ON} scenario) and **0.7** (R_{OFF} scenario).

What do we learn from this exploratory study?

The expected geoneutrino signal is $\mathbf{S_{LOC}} = 17.4^{+3.3}_{-2.8}$ TNU from the 6 tiles, to compare with $\mathbf{S_{TOT}} = 39.7^{+6.5}_{-5.2}$ TNU.

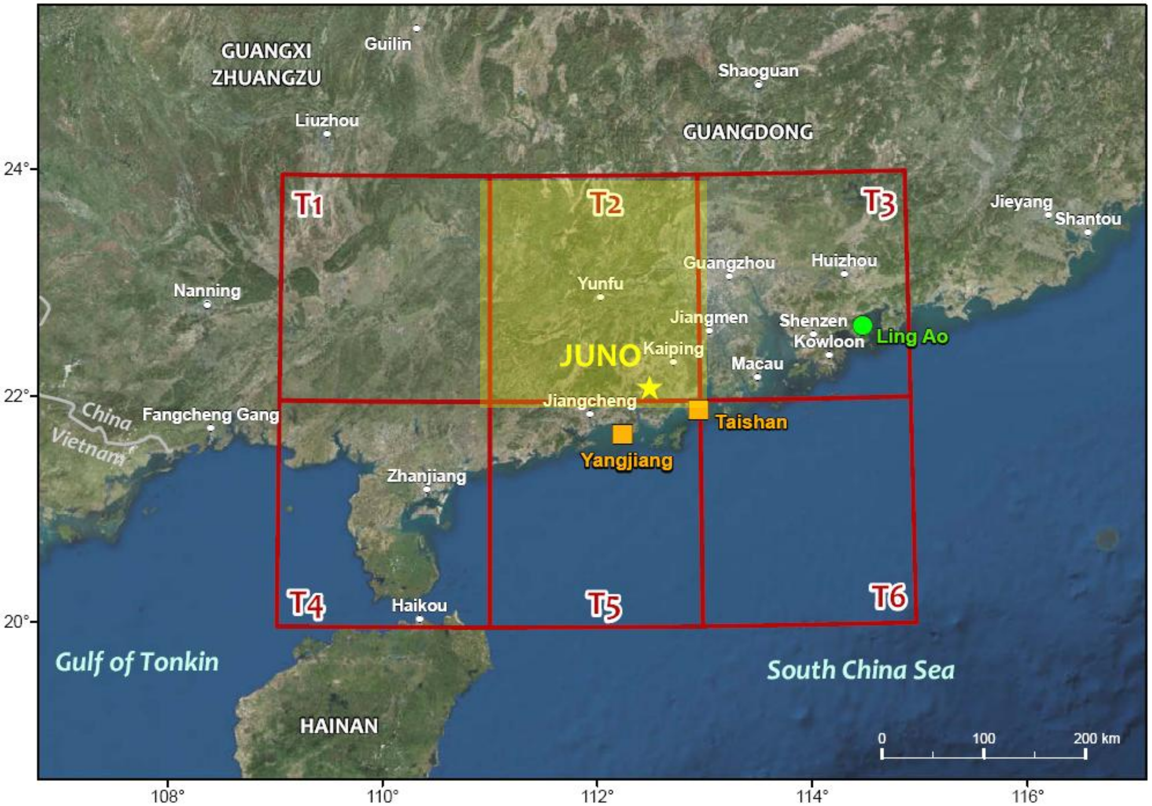

Tile	S (U+Th)	Percentage
T1	$0.5^{+0.1}_{-0.1}$	3.0
T2	$10.8^{+2.1}_{-1.8}$	62.1
T3	$1.5^{+0.3}_{-0.3}$	8.6
T4	$0.4^{+0.1}_{-0.1}$	2.2
T5	$3.2^{+0.6}_{-0.5}$	18.2
T6	$1.0^{+0.2}_{-0.2}$	5.9

The U and Th in T2 produces $\mathbf{10.8^{+2.1}_{-1.8}}$ **TNU**. The **70%** comes from the thick **UC** characterizing this tile which needs a refined geophysical and geochemical model.

Personal conclusion

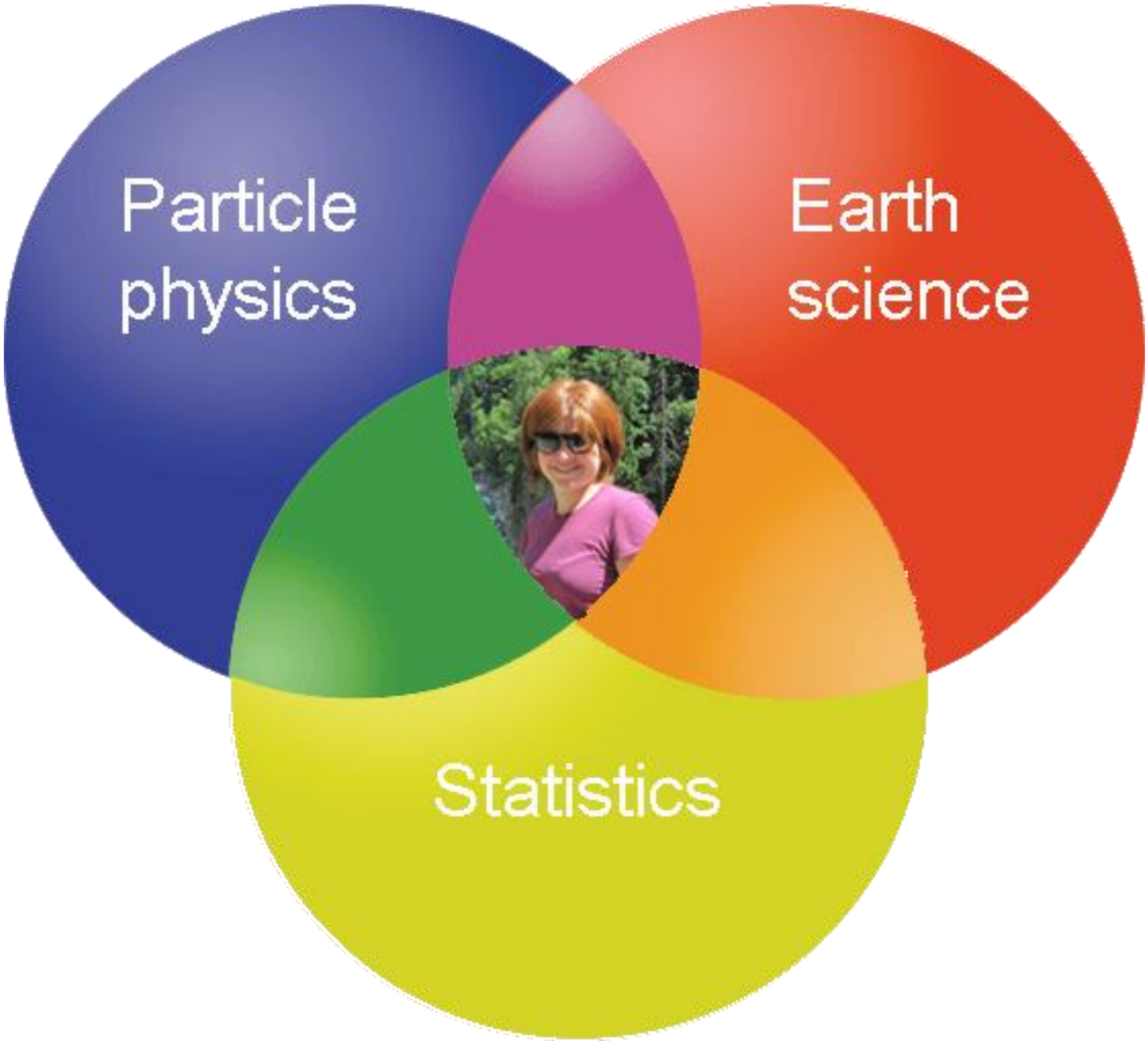

Personal conclusion

$$P_{ee}(E_{\bar{\nu}_e},\vec{r}) = \cos^4(\theta_{13})\left(1-\sin^2(2\theta_{12})\sin^2\left(\frac{\delta m^2 \vec{r}}{4E_{\bar{\nu}_e}}\right)\right)+\sin^4(\theta_{13})$$

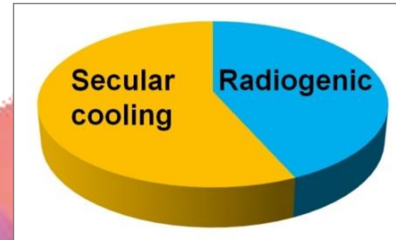

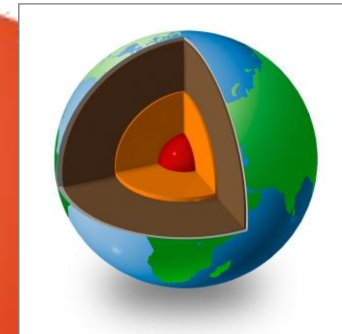

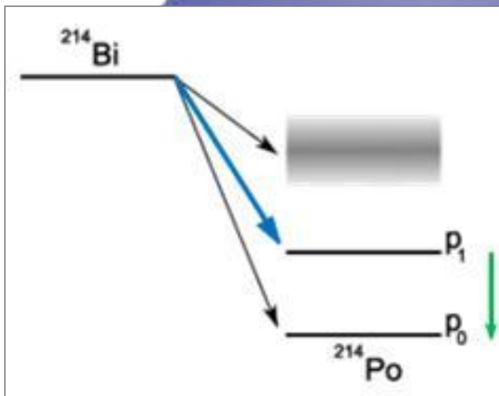

I see advancing science in the intersection of particle physics, earth science and statistics.

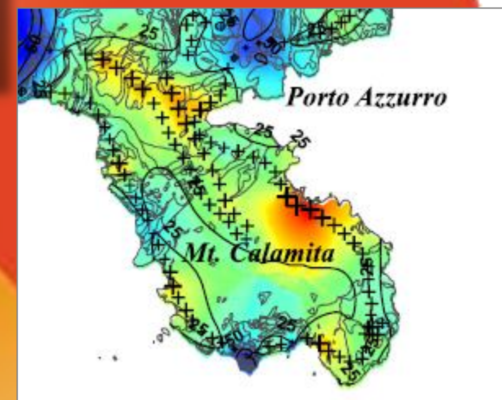

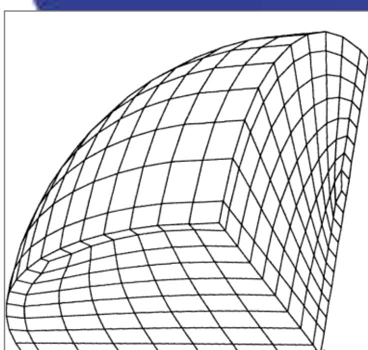

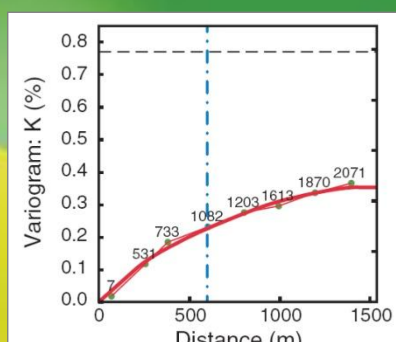

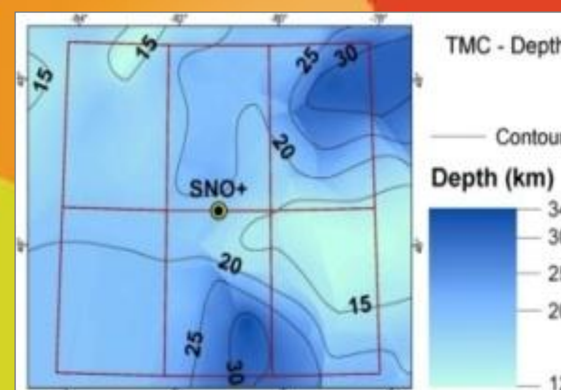

Pubblications

• Kaçeli Xhixha M., Albèri M., Baldoncini M., Bezzon G. P., Broggini C., Buso G.P., Callegari I., Casini L., Cuccuru S., Fiorentini G., Guastaldi E., Mantovani F., Mou L., Oggiano G., Puccini A., Rossi Alvarez C., Strati V., Xhixha G. and Zanon A. Uranium distribution in the Variscan Basement of Northeastern Sardinia. Journal of Maps, (2015) 1-8. DOI: 10.1080/17445647.2015.1115784

• Xhixha, G., Alberi, M., Baldoncini, M., Bode, K., Bylyku, E., Cfarku, F., Callegari, I., Hasani, F., Landsberger, S., Mantovani, F., Rodriguez, E., Shala, F., Strati, V., Kaçeli Xhixha, M., Calibration of HPGe detectors using certified reference materials of natural origin." Journal of Radioanalytical and Nuclear Chemistry. DOI 10.1007/s10967-015-4360-6

• Tushe, K. B., Bylyku, E., Bylyku, E, Xhixha, G., Dhoqina, P., Daci, B., Cfarku, F., Xhixha, M. K., Strati, V. *First Step Towards the Geographical Distribution of Indoor Radon in Dwellings in Albania*. Radiat Prot Dosimetry. 2015 DOI: 0.1093/rpd/ncv494.

• Xhixha G., Baldoncini M., Callegari I., Colonna T., Hasani F., Mantovani F., Shala F., Strati V., Xhixha Kaçeli M.. *A century of oil and gas exploration in Albania: Assesment of Naturally Occuring Radioactive Materials (NORMs)*. Chemosphere 139(0) (2015) 30 - 39. DOI: http://dx.doi.org/10.1016/j.chemosphere.2015.05.018.

• Strati V., Baldoncini M., Callegari I., Mantovani F., McDonough W.F., Ricci B., Xhixha G. *Expected geoneutrino signal at JUNO*. Progress in Earth and Planetary Science 2(1) DOI: 10.1186/s40645-015-0037-6.

• Baldoncini M., Callegari I., Fiorentini G., Mantovani F., Ricci B., Strati V., Xhixha G. *Reference worldwide model for antineutrinos from reactors*." Physical Review D 91(6): 065002 (2015). DOI: 10.1103/PhysRevD.91.065002

• Strati, V., Baldoncini, M., Bezzon, G. P., Broggini, C., Buso, G. P., Caciolli, A., Callegari, I., Carmignani, L., Colonna, T., Fiorentini, G., Guastaldi, E., Kaçeli Xhixha, M., Mantovani, F., Menegazzo, R., Mou, L., Rossi Alvarez, C., Xhixha, G., and Zanon, A. *Total natural radioactivity, Veneto (Italy)*. Journal of Maps, 11(4) (2015) 543 - 551. DOI: http://dx.doi.org/10.1080/17445647.2014.923348

• Huang Y., Strati V., Mantovani F., Shirey S. B. and McDonough W. F. *Regional study of the Archean to Proterozoic crust at the Sudbury Neutrino Observatory (SNO+), Ontario: Predicting the geoneutrino flux.* Geochemistry, Geophysics, Geosystems, 15 (2014) 3925–3944, doi:10.1002/2014GC005397

• Guastaldi E., M. Baldoncini, G. Bezzon, C. Broggini, G. Buso, A. Caciolli, L. Carmignani, I. Callegari, T. Colonna, K. Dule, G. Fiorentini, M. Kaçeli Xhixha, F. Mantovani, G. Massa, R. Menegazzo, L. Mou, C. Rossi Alvarez, V. Strati, G. Xhixha, A. Zanon, *A multivariate spatial interpolation of airborne γ-ray data using the geological constraints*. Remote Sensing of Environment, 137 (2013) 1-11. DOI: 10.1016/j.rse.2013.05.027

• Callegari I., G.P. Bezzon, C. Broggini, G.P. Buso, A. Caciolli, L. Carmignani, T. Colonna, G. Fiorentini, E. Guastaldi, M.K. Xhixha, F. Mantovani, G. Massa, R. Menegazzo, L. Mou, A. Pirro, C.R. Alvarez, V. Strati, G. Xhixha, A. Zanon. *Total natural radioactivity, Tuscany, Italy*. Journal of Maps, 9 (3) (2013) 438 - 443. DOI: 10.1080/17445647.2013.802999.